A COLLABORATIVE STUDY:
MARINE GEOPHYSICAL INVESTIGATION
OF THE PUERTO RICO TRENCH

EW9605

BY

UNIVERSITY OF PUERTO RICO
INSTITUTE FOR GEOPHYSICS, UNIVERSITY OF TEXAS AT AUSTIN
UNIVERSITY OF SOUTHERN CALIFORNIA

PRELIMINARY SHIPBOARD SCIENTIFIC RESULTS
(PLEASE RESTRICT DISTRIBUTION TO UPR, UTIG AND USC PARTICIPANTS)

TABLE OF CONTENTS

CHAPTER 1. INTRODUCTION AND HISTORY OF EW96-05 PROJECT

This report describes the methods and preliminary results of a marine geophysical (HMR1, single-channel seismic, gravity and magnetics) cruise EW96-05 aboard the R/V MAURICE EWING to the Puerto Rico trench during June 15, 1996 to July 8, 1996. This report is accompanied by the UNOLS Research Vessel Cruise Assessment Form and the UNOLS Cruise Report/Ship Utilization Data Report.

The Puerto Rico trench and northern margin of the island of Puerto Rico occupy a zone of tectonic transition between subduction tectonics of the Lesser Antilles island arc and strike-slip tectonics of the Septentrional-Cayman trough left-lateral strike-slip fault system to the west (Fig. 1, inset). Obliquely colliding high-standing bathymetric features on the downgoing North America plate beneath the Caribbean plate make this region a promising area to investigate the time-transgressive deformational effects of fracture zone and aseismic ridge collisional events at margins of highly oblique convergence. (Fig. 1.1).

The project was initiated by Grindlay, Mann and Dolan with a proposal submitted to the Marine Geology and Geophysics program of the National Science Foundation's Ocean Sciences Division in the Spring of 1994. Ship time and use of a magnetometer, single-channel seismic system and gravimeter were requested on the R/V ENDEAVOR through a subcontract with the University of Rhode Island. Use of the HMR1 system was requested through a subcontract with the Hawaii Mapping Research Group at the University of Hawaii. The NSF proposal and accompanying subcontracts were initially turned down.

A revised version of the NSF proposal submitted by UPR-UTIG-USC and accompanying subcontracts from URI and HMRG were submitted in fall of 1994 and approved for funding pending availability of ship time. In spring of 1995 due to UNOLS ship scheduling logistics the program was scheduled for June 1996 on the R/V MAURICE EWING and a subcontract from LDEO replaced the URI subcontract. Funding to start the UPR-UTIG-USC program and LDEO and HMRG subcontracts became available on April 15, 1996 and extends through 1999.

Science Party

The science party of EW96-05 consisted of 19 individuals from seven different institutions (for an alphabetical listing of names and addresses see Appendix V):

University of Puerto Rico, USA
Dr. Nancy Grindlay, Co-Chief-scientist
Ms. Frances Delano, undergraduate student
Mr. Wilfredo Rosado, undergraduate student

University of Texas at Austin, Institue for Geophysics (UTIG) and Department of Geological Sciences (DOGS), USA
Dr. Paul Mann, Co-Chief scientist, UTIG
Mr. Steve Muszala, Graduate research assistant, DOGS, PhD aspirant
Mr. Jean-Paul van Gestel, Graduate research assistant, DOGS, PhD aspirant

University of Southern California, USA
Dr. James Dolan, Co-Chief scientist

Spanish Institute of Oceanography, Madrid, Spain
Dr. Araceli Munoz

West Virginia Weslyan College, USA
Mr. John Charles, III

Lamont Doherty Earth Observatory of Columbia University, USA
Mr. Chris Leidhold, Science Officer
Mr. John DiBernardo, Technician (airguns)
Mr. Carlos Alvarez, Technician (airguns)
Mr. Paul Osgard, Technician (electrical)
Mr. William Robinson, Computer systems manager
Mr. Michael Wittreich, Technician (airguns)

University of Hawaii, HMR1 group
Dr. Bruce Appelgate, MR1 Chief of operations
Mr. Steve Tottori, MR1 Engineer
Ms. Karen Sender, MR1 Data processor
Ms. Tina Mueller, MR1 Data processor

Crew

Captain James O'Loughlin
Mr. Stan Ziegler, Chief mate
Mr. Mark Landow, Second mate
Mr. Jeff Sylvia, Third mate
Mr. Larry Barros, Boatswain
Mr. John Shank, A/B
Mr. Dermot Taaffe, A/B
Mr. David Wolford, A/B
Mr. Robert Hagg, O/S
Mr. Rickey Wyatt, O/S
Mr. Albert Karlyn, Chief Engineer
Mr. Sport Moran, 1st Engr.
Mr. Todd Soper, 2nd Engr.
Mr. Paul Morric, 3rd Engr.
Mr. Edward Shimel, Oiler
Mr. Guillermo Uribe, Oiler
Mr. William Osborn, Oiler
Mr. John Schwartz, Electrician
Mr. Tim Hummel, Steward
Mr. Richard Craig, Cook
Mr. Joseph LoPrinzi, Utility

Research Vessel Specifications and Equipment Used for Science Operations

The R/V MAURICE EWING is a 72.750 meter long oceanographic research vessel with a gross tonnage of 1978. It is owned and operated by Lamont Doherty Earth Observatory, Columbia University. The R/V EWING was built by Marine Industrie Ltde of Quebec Canada in 1983 and was converted to oceanographic research use in 1990. It can reach and maintain underway speeds of 12 kts, and it has a berthing capacity for up to 50 persons.

The R/V EWING is equiped with a Bell Aerospace BGM-3 gravimeter, Varion proton precession magnetomer, DMS 2000 SCS seismic system and Hydrosweep multibeam bathyetric system. In this study the MR1 sidescan sonar system including launching/recovery system and tow winch were shipped from Hawaii and bolted into the back deck. The SCS streamer and air-gun array, magnetometer, and MR1 were all deployed and recovered from the fantail.

The Main Science Lab on Deck C was used for watchstanding and as a general work area. The wet staging area on Deck C was used to as an electronics workshop for testing and repairing the MR1 system and as the primarly location of MR1 data processing.

Acknowledgements

The dedication and hard work of Captain O'Laughlin, the crew, science officer and technicians aboard the R/V EWING during cruise EW96-05 are gratefully acknowledged. The professional ship handling and seamanship were instrumental to the scientific research conducted during the cruise.

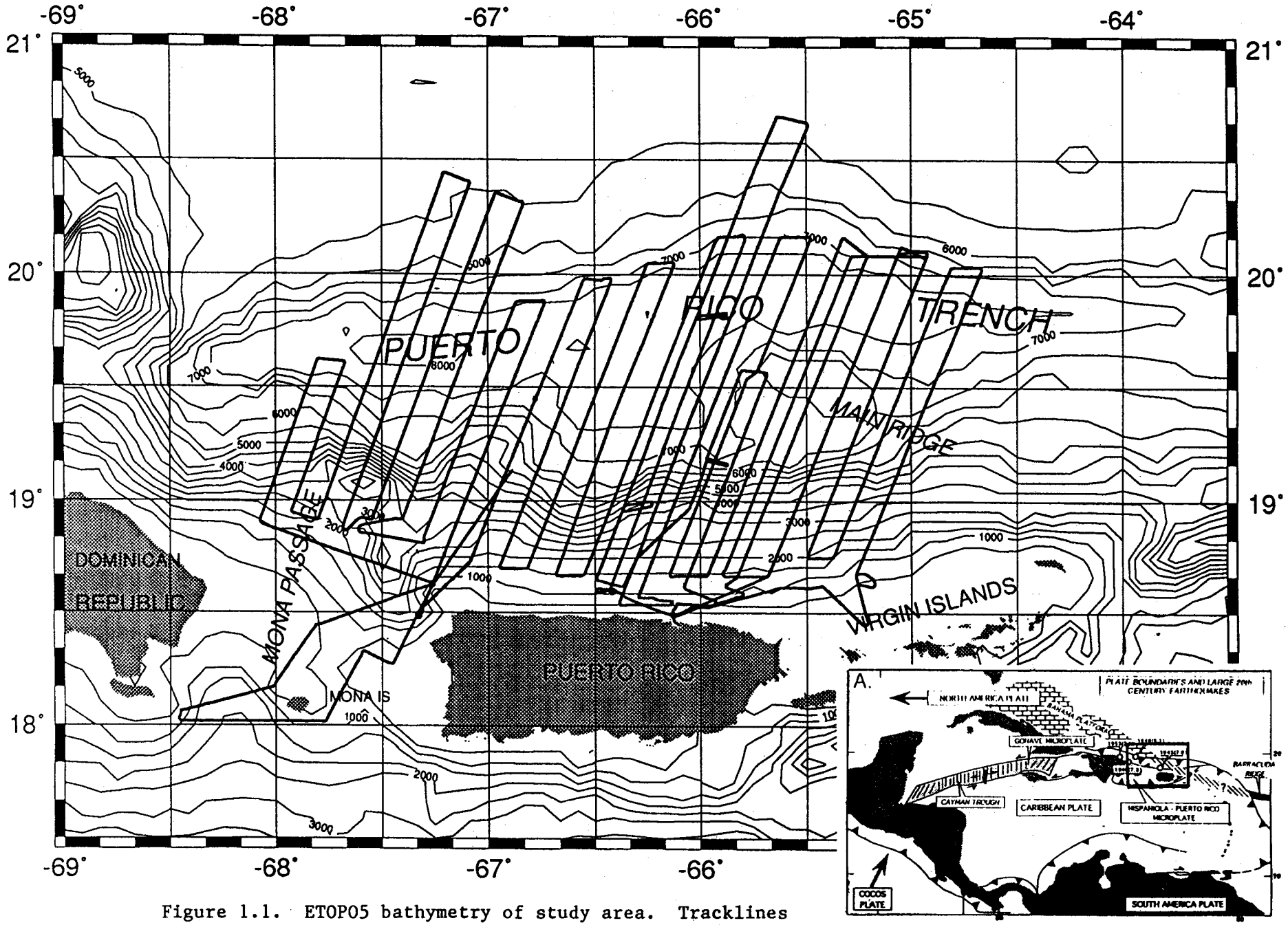

Figure 1.1. ETOP05 bathymetry of study area. Tracklines for JD 167-188 shown as thick black lines. Inset shows regional setting of study area.

CHAPTER 2. COMPARISON OF PROPOSED OBJECTIVES OF EW96-05 WITH A PRELIMINARY ANALYSIS OF THE DATA

by Paul Mann, Nancy Grindlay and James Dolan

The major objective of this high-resolution sidescan/bathymetric (MR1) and geophysical (magnetic, gravity and SCS data) investigation of the Puerto Rico trench and northern slope of the island of Puerto Rico is to systematically map the zone of active collision between obliquely subducting aseismic ridges and a plate boundary margin. The Main Ridge area of the Puerto Rico trench is selected as the focus of this study because this area appears to represent the zone of active collision along this segment of the North American-Caribbean plate boundary (McCann and Sykes, 1984) (Fig. 2.2A). The character of this collision zone is critical for understanding patterns of ancient deformation in a postulated post-collisional zone from the Main Ridge to the Lesser Antilles Islands as well as understanding the present-day zone of deformation and related seismicity. Our survey area includes a postulated pre-collisional area to the west of the Main Ridge in order to better understand transpressional and strike-slip deformation unrelated to collision.

An added complexity to the understanding of this area involves the post-collisional effects of the passage of the southeastern extension of the Bahama platform. The active collision of the Bahama platform is presently occurring along the northeastern margin of Hispaniola (Dolan and Wald, in press) so it is reasonable to assume that this zone of left-lateral oblique slip that the Puerto Rico margin experienced this collisional event in the late Neogene and is now in a state of post-collisional adjustment.

Below we list verbatim our proposed objectives followed by an evaluation of these objectives based on the preliminary results of EW96-05.

Proposed Objective 1: Does the Main Ridge in the Puerto Rico Area Demarcate a Zone of More Deformed Seafloor to the East From a Zone of Less Deformed or Undeformed Seafloor to the West?

Studies of obliquely subducting ridges and seamounts along the Tonga Trench (Ballance et al., 1989), and orthogonally subducted seamounts and ridges at the Japan and Peru convergent margins (von Huene and Lallemand, 1990) show accelerated tectonic erosion of the forearc due to the fracturing and shearing of arc substrate rocks as they are lifted up by the colliding bathymetric high, and then left to collapse as the ridge moves away. This wave of vertical tectonism travels along the landward trench slope lifting it and then letting it subside again leaving an extended or collapsed terrain in its "wake". von Huene et al. (1995) have recently shown spectacular examples using Hydrosweep bathymetry of furrows up to 55 km long in the Costa Rica accretionary prism that mark the collapsing paths of subducting seamounts.

A time-transgressive zone of deformation caused by the oblique subduction of the Barracuda Ridge has been proposed by McCann and Sykes (1984) mainly on the basis of teleseismic data and widely spaced SCS lines. Figure 2.2A and B summarizes the relationship of obliquely subducting ridges to the proposed forearc basins of McCann and Sykes (1984). According to their model, the forearc basins west of the Main Ridge have not been affected by shallow subduction of Barracuda-Main Ridge and therefore contain undisturbed sedimentary rocks deposited in an arcuate but discontinuous "forearc basin" inferred from the central part of the Lesser Antilles to the Puerto Rico trench area. Main Ridge lies oblique to the ridges and basins that make up the forearc of the inner wall of the Puerto Rico trench. The Main Ridge interrupts these features and they are not observed east of where it intersects the arc. According to McCann and Sykes (1984) as the Main Ridge passed beneath the sediments on the inner wall of the trench, where it disrupted "well developed structures and left a chaotic terrain in its wake".

To illustrate this hypothesis, they presented two SCS lines collected by the R/V CONRAD in the early 1970s. Line A-A' in Figure 2.2B is a north-south line which according to McCann and Sykes (1984) is a "classical ridge basin sequence in the forearc region" that has not yet been affected by the oblique subduction of the Main-Barracuda Ridge. The "classic forearc structure" they refer to includes: 1) the Puerto Rico trench; 2) the "Main Ridge", which was first named by Ewing et al. (1965)(Fig. 2.1); 2) an "Outer Arc Ridge", called the "Median Ridge" by Ewing et al. (1965), and lying to the west of the Main Ridge; and 3) a "Forearc Basin" called the "Elevated Plain" by Ewing et al. (1965) because it forms a turbidite-filled basin south of the Main Plain of the Puerto Rico trench but a shallower depth.

The Forearc basin/Elevated Plain is filled with about 0.5 seconds of highly reflective turbidites tilted to the southwest away from the Median Ridge. This basin acts as a channel for turbidites derived from the Puerto Rican shelf margin. These turbidites flow from the Elevated Plain into the Main Plain of the Puerto Rico trench through an "Abyssal Gap" identified by Ewing et al. (1965) at the western end of the Median Ridge.

In a second line, B-B', McCann and Sykes emphasized a "ridge-trough topography" between the Main Ridge and the trench whose troughs are inferred to be young in age because they do not contain young turbidites. This area is inferred to be the chaotic area formed in the wake of the obliquely subducting Main Ridge.

We proposed to collect higher resolution and synoptic sidescan imagery and seismic profiles at 14 km spacing across a zone east of the Main Ridge (after deformation), on the Main Ridge (zone of active collision) and west of the Main Ridge (zone as yet undeformed by the collision event). The higher resolution MR1 sidescan images and bathymetry combined with SCS profiles could potentially allow us to map convergent structures at the front of the ridge and extended or collapse structures in the "wake" of the ridge along with furrows marking the path of the bathymetric high along the base of the accretionary wedge.

Evaluation of Objective 1 Based on Preliminary EW96-05 Results:

Our closely spaced SCS lines reveal the distribution of turbiditic sediments and the along-strike continuity of the Main and Median Ridges and can therefore be used to evaluated the McCann and Sykes (1984) model that is shown in Figure 2.2A and B.

Landward projection of the Main Ridge. The Main Ridge is first seen as a rise on the slope of the Virgin Islands platform on Line 14 at the eastern limit of the study area. As predicted in the McCann and Sykes (1984) model, this ridge projects towards Anegada, the easternmost island in the Virgin Islands, which they interpreted as a surficial bulge above the bathymetric high of the subducted Main-Barracuda ridge (Fig. 2.2A). This island is the only island in the Virgin Islands exhibiting evidence for late Quaternary uplift (McCann and Sykes, 1984).

Post-collisional area. On Line 14 on Figure 2.4A, a "ridge trough topography" with no turbidite fill is present north of this rise on the slope and leads to the Puerto Rico trench, a narrow zone also lacking a turbidite fill. The crest of the Main Ridge reaches maximum elevation on Line 9 and progressively plunges in elevation to the west on Lines 8 through 4 (Fig. 2.4B). On Line 19, the Main Ridge disappears as a discrete topographic high and the Median Ridge appears with the strongly southwestwardly tilted turbidites of the Forearc basin/Elevated plain along its southwestern flank (Fig. 2.4B). The uplift of the Median Ridge and the strong tilting seen in the adjacent Elevated Plain suggests that this deformation may be linked to the disappearance and oblique subduction of the Main Ridge at this location on the Puerto Rico trench presumably by oblique subduction.

However, the argument by McCann and Sykes (1984) that the Median Ridge-Elevated Plain represents a "classic forearc basin" may be flawed for three reasons:

• the Median Ridge-Elevated Plain is highly oblique to the Puerto Rico trench and cannot be traced more than 30 km along strike. If these features formed as "classic forearc features" they would be expected to extend for greater distances along the strike of the Puerto Rico trench, particularly if the direction of plate convergence is as large (S70°W) as predicted by McCann and Sykes (1984). A more likely explanation based on the seismic lines shown in Figure 2.4 is that the Median Ridge is a highly localized response to oblique subduction of the Main Ridge.

• the turbidite fill of the Elevated Plain is dependent on the location of this area downslope from the Puerto Rico shelf (Ewing et al., 1965). The Median Ridge shields the area along its northeastern flank from turbidite sedimentation. While its possible that this northeastern flank lacks sediment because of its post-collisional setting, it is also possible that these differences are related only to the blockage of turbidite sedimentation by the Median Ridge itself.

• Masson and Scanlon (1991) show from GLORIA data that almost all of the tectonic elements of the basin and ridge province to the east and west of the Main Ridge are distinctly oblique to the trench, a situation not seen in other forearcs, even in areas of highly oblique convergence such as off the western Aleutians.

Proposed Objective 2: What is the Nature of the Main Ridge?

MR1 data and seismic profiles may reveal that Main Ridge represents the deformation produced by a subducted fracture zone on the downgoing North America plate that is continuous with fracture zones of the southeastern Bahama Platform mapped in 1989 by Dolan et al. using the SeaMARC II sidescan system. We favor this interpretation and its corollary - a regional decollement separating the top of the downgoing bathymetric high from a thin flap of the overriding Caribbean plate. Alternatively, the Main Ridge could be a localized zone of uplift in the overriding Caribbean plate between en echelon stepping strike-slip faults as proposed by Masson and Scanlon (1991) (cf. fig. 3B) or a fragment of the metamorphic basement rocks of the Caribbean that has been uplifted along a reverse or thrust fault. At the time of the proposal, we preferred the first interpretation mainly because the gravity anomaly of the Main Ridge aligns so well with fracture zone trends on the downgoing plate in both the Bahamas and Lesser Antilles (Fig. 2.2A).

Bathymetric data in combination with gravity data will provide information about the subsurface density structure in the region to further constrain the nature of the Main Ridge. Magnetic anomalies have been observed in association with aseismic ridges and fracture zones traces in the region (Geddes and Dennis, 1964; Griscom and Geddes, 1966). If the Main Ridge is indeed continuous with the southeastern Bahama Platform, a magnetic lineament may be traced between these features (Fig. 2.2A). Many of the existing MCS lines in the region have had very limited processing. We propose to migrate some existing MCS lines to help define the upper plate from the lower plate and examine deeper structures in the vicinity of the Main Ridge.

Evaluation of Objective 2 Based on Preliminary EW96-05 Results:

Figure 18.1.10 compares the position of a fracture zone mapped by Treadgold (1985) using reflection and refraction data and a topographic high mapped by Leonardi (1981, unpublished data) using Seabeam? bathymetric mapped (map published by McCann and Sykes, 1984). On EW96-05, we surveyed this ridge using SCS (Lines 26, 27 and 28) and MR1 sidescan and confirmed its location and dimensions of about 15 km wide and with about 600 m of bathymetric relief above the surrounding seafloor (Figure 18.1. 3A and B).

As pointed out by McCann and Sykes (1984), the later bathymetric high and the Main Ridge are collinear across the Puerto Rico trench. The fracture zone mapped by Treadgold (1985) is about 30 km north of the bathymetric high and projects into the ridge-trough topography northeast of the Main Ridge (cf. Lines 5, 6, 7 on Figure 3). The inference that the Main Ridge is formed by a subducted fracture zone that presumably underlies the bathymetric high mapped by Leonardi (1981) therefore is consistent with the data collected on this cruise.

The presence of the eastern fracture zone may explain the abrupt change in strike of normal faults in Atlantic seafloor at 65°45'W. As noted by Masson and Scanlon (1991) this change mirrors a change in the trend of the trench which occurs just outside the eastern edge of their Gloria study area. The zone of normal faulting on the bending Atlantic plate also changes character at this point. To the west its made up of two major fault scarps, but to the east it is much broader and is made up of a complex horst and graben province. Detailed sections across the turbidite fill of the Puerto Rico trench reveal what appear to be strike-slip faults nucleating on the faults separating the downbending basement highs of Atlantic crust. The long straight, ENE-striking faults in the Atlantic crust of the western trench may therefore be in the process of being reactivated as strike-slip faults.

Proposed Objective 3: What is the Relation of Thrust Faults and Strike-Slip Faults in the area of the Main Ridge?

Do strike-slip faults including the main trace of the North America-Caribbean plate boundary (Septentrional/Escarpment fault system) terminate at the Main Ridge or do they extend eastwards across the zone of active collision? In the former case the collision would have a greater effect in transforming the character of the plate boundary than in the latter case.

The GLORIA sidescan data collected over the northern margin of Puerto Rico was incomplete and of insufficient resolution to image the East Septentrional/Escarpment fault system. The proposed survey will provide complete coverage of the fault system from landfall in Hispaniola, through the Mona Passage, north of Puerto Rico and the Virgin Islands to its intersection with the Puerto Rico trench/Lesser Antilles subduction zone around 63°W. In addition, we will be able to determine the relation between the active fault systems and areas of submarine slump scars (e.g. Schwab et al., 1991) and identify areas of potential instabilities along the north coast of Puerto Rico and the Virgin Islands. One possibility is that these type of slumps are triggered by major earthquakes like the one that occurred between A.D. 1150-1230 in Hispaniola (Prentice et al, 1993) The seismic reflection data will provide a depth perspective of the faults imaged with the sidescan data to make it possible to define fault geometries and characterize the style of recent faulting along the length of the fault system.

Evaluation of Objective 3 Based on Preliminary EW96-05 Results:

Our last line of the cruise followed what appears to be the eastward continuation of the Septentrional fault zone along the base of the scarp formed by the subsided carbonate margin. A sketch map based on a preliminary MR1 mosaic is provided in Figure 2.5.

Three distinct segments of the fault all display characteristics of an active left-lateral fault zone. Fine scale alternation of releasing and restraining bends on the central segment of the fault establishes its left-slip character along with the orientation of the larger transtensional segments bounding it to the east and west. Only a small part (~10 km) of this fault system was recognized on the Gloria mosaic of Masson and Scanlon (1991).

The western and eastern segments strike 070 to 080 and exhibit a transtensional character. The central segment strikes 080 to 090 and exhibits a pure strike-slip character. The ENE-striking western and eastern segments may control similarly trending segments of the Puerto Rico shelf margin to the south. For example, the western transtensional fault is north of

the ENE-trending eastern edge of the megaslump area described in detail by Schwab et al. (1991). The eastern transtensional fault trends parallel to the more ENE edge of the Virgin Islands Platform.

The eastern transtensional fault segment clearly crosscuts the Main Ridge. The point of intersection corresponds to a bathymetric saddle crossing Main Ridge in an ENE orientation that is visible on maps as crude as the ETOPO-5 bathymetric map with 200 m contours. The apparent lack of offset of the bathymetric trend of the Main Ridge at this saddle suggests that: 1) either the fault is young and offset has not been significant; or 2) that the Main Ridge is a topographic reflection of a topographic feature (fracture zone?) on the underthrust plate that is largely unaffected by strike-slip displacements on the overriding Puerto Rico margin.

Proposed Objective 4: Which Tectonic Model Best Explains the Origin of the Puerto Rico Trench?

We propose sidescan mapping, SCS profiling and migration of existing MCS lines to "test" or at least show the agreement or disagreement of these data with a dizzying array of tectonic models for the formation of the Puerto Rico trench". The main ideas and implications of the models are summarized below and compared with the types of data previously collected and proposed in this study. We emphasize that the origin of the Puerto Rico trench remains enigmatic because previous studies have not been systematic but relied on a hodgepodge of previous and often non-systematic studies.

Model One: The Puerto Rico trench formed in an island arc setting by southwestward subduction of the North America plate beneath the Caribbean plate (McCann and Sykes, 1984; McCann and Pennington, 1990). This model invokes oblique convergence to explain what appears to be a continuous Benioff zone traceable from the Lesser Antilles to eastern Hispaniola. If this hypothesis is correct, we would expect to see structures common in accretionary prisms striking about N135° in young sediments of the Puerto Rico trench. Heubeck and Mann (1991) point out onland geologic inconsistencies in the greater amount of convergence required by this model along the length of the entire plate boundary while Dillon and Coleman (in review) note that this model does not explain the abrupt westward termination of the Benioff zone in eastern Hispaniola. Previous GLORIA studies are instructive but not conclusive on the orientations of active folds and faults in the Puerto Rico trench Earthquake focal mechanisms suggest a range of oblique convergence from N50°-85° (Dolan and Wald, in press) but this results from strain partitioning of strike-slip motion.

Model Two: The Puerto Rico trench formed by transtension (Larue et al., 1990; Larue and Ryan, 1990; Speed and Larue, 1991). This model attributes the depth of the trench, the large reentrant in the plate boundary, the gravity anomaly, and the 4 km of late Neogene subsidence of the southern margin of the Puerto Rico trench to transtension along the plate boundary.

Masson and Scanlon (1991) and Larue (in press) identified faults along the western part of the Main Ridge and the south slope of the Puerto Rico trench but not at the base of the Puerto Rico island slope. The results of this survey suggests faults at the base of the slope. A simple model for the formation of the Puerto Rico trench would consist of a large extensional stepover zone developed between the two overlapping and active strike-slip faults. The lack of compressive deformation in the central and eastern parts of the turbidite-filled Main Plain of the Puerto Rico trench suggests that this feature may be transtensional. Transpressional folding is only present in the western Puerto Rico trench at the foot of the Mona block, a possible restraining bend along the Septentrional fault zone (see below). Masson and Scanlon (1991) point out that the best evidence for subduction is the seismicity and presence of a subducted slab. Most other lines of geological and geophysical evidence, including those collected during this cruise, favor a strike-slip origin.

Model Three: The Puerto Rico trench and associated Benioff zone formed in an island arc setting to the east in the Lesser Antilles area and was rafted westward to its present position on east-west strike-slip faults (Schell and Tarr, 1978; Calais and Mercier de Lepinay, 1991). Transported subducted lithosphere of the North America plate survives to the west in their words because it is "above the critical melting depth". If this model is correct, we would expect to see remnant accretionary wedge structures crosscut by younger east-west strike-slip faults and the downgoing plate "disconnected" by vertical strike-slip faults from the adjacent Benioff zone. A previous SeaMARC II investigation has identified strike-slip faults on the south slope of the Puerto Rico trench that appear to be continuous with known strike-slip faults in Hispaniola.

Model Four and preferred model at the time of the proposal submission: The Puerto Rico trench formed by the oblique collision of an obliquely subducting Atlantic fracture zone. Dolan and Wald (1994) recently proposed that the 4 km of late Neogene subsidence and the reentrant in the northern Puerto Rico slope occurred in response to removal of topographic support for the Puerto Rico shelf provided by underthrusting fracture zones and overlying carbonate banks as the colliding ridges swept westward through time. This model would predict localized and time transgressive subsidence tied to specific fracture zones shown in Figure 2.3A.

Model Five. The Puerto Rico trench formed in response to "deep plate collision" or mantle interaction between south-dipping North America slab depressed by a north-dipping Caribbean slab as shown by serial profiles of seismicity through Puerto Rico (Dillon and Coleman, in review). Depression of the North America plate caused regional subsidence of the Puerto Rico slope that would contrast to the more localized subsidence predicted in Model Four above.

Evaluation of Objective 5 Based on Preliminary EW96-05 Results:

The uplift, subsidence and deformation history of the Oligocene-Early Pliocene carbonate platform of the Virgin Islands, Puerto Rico and the eastern Dominican Republic provides an excellent test of the timing and origin for the formation of the Puerto Rico trench. Previous workers like Moussa et al. (1987)(See chapter 18 for review of Moussa et al.) and Birch (1986) have pointed this out but have failed to provide a regionally consistent model because their data is limited to the margin in central and northwestern Puerto Rico.

New SCS data from EW96-05 has increased this coverage over an along strike distance of 200 km. Four representative SCS lines covering an along-strike distance of 200 km and crossing the platform at a high angle (020) are interpreted on Figure 2.7. It should be emphasized that these interpretations and correlations were done quickly and are subject to revision. Below is a brief summary of new interpretations of this margin based on these data:

1. The carbonate platform may be much thicker and younger beneath the offshore area than assumed by Moussa et al. (1987). The middle unit of Moussa et al. (1987) has somewhat regular internal reflectors and some reflectors have apparent landward dips suggesting listric faulting (Fig. 2.6A). Ages and compositions are poorly constrained because they interpreted this unit as pinching out in a data gap less than 35 km from the CPR-4 well (Fig. 2.6A). They interpret the top of this unit to be the base of the San Sebastian Formation, a Middle Oligocene transgressive deposit found onland to be above folded rocks of Eocene age. By a process of elimination they suggest an age of late Middle Eocene to Middle Oligocene for the middle unit. This unit would therefore have no onshore correlatives.

An alternative interpretation is that the base of the San Sebastian Formation is at the base, not the top, of their middle unit. This would mean that the middle unit is a seaward-thickening offshore part of the late Oligocene to early Pliocene carbonate margin. This interpretation is consistent with the similar seismic character and dip of the middle and upper

units. The geometry of the middle unit suggests that the thicker part of the platform is a greatly expanded section present only in condensed form in the CPR-4 well.

Another argument for this revised interpretation is the fact that the middle unit is unfolded. Onland studies in Puerto Rico have established that rocks of Eocene to Early Oligocene age beneath the Middle Oligocene San Sebastian Formation are folded and thrusted (cf. Dolan et al., 1991, for a review). The lack of a significant discordance at the contact between the upper and middle units indicates that no major folding event occurred at this time.

Larue and Berrong (1991) have emphasized that the unfolded nature of the middle unit is not consistent with Pindell and Barrett's (1990) model for fold-thrust deformation of the Puerto Rico arc during its collision with the Bahama platform. They argue that a Bahama collision event would produce progressively deformed offshore sections rather than the undeformed but tilted section seen on their line. However, if the deposition of their middle unit postdates collision then the fold-thrust model could still be viable.

In their MCS line tied to the Toa Baja well they infer a down-to-the south-vertical fault offsetting Eocene basement near the coast. This fault effectively raises the level of their Eocene basement in the offshore area. This inferred fault throw may have led to a miscorrelation between Eocene rocks that are present at much deeper levels in the offshore areas. The down-to-the-north fault interpretation in the Moussa et al. (1987) line seems a much more likely explanation for the greatly expanded thickness of the middle unit. More work is needed to correlate the Moussa et al. fault with the fault seen on these data.

2. The carbonate margin contains a major, coast parallel but offshore barrier reef complex that is poorly known because it lies at great depth beneath the previously studied area of central and northwest Puerto Rico. The interpretation of Moussa et al. (1987) and Larue and Berrong (1991) is that the carbonate margin is a planar ramp that dips offshore and exhibits no major vertical relief. There is a suggestion of a reefal buildup at about 2.5 seconds on the Moussa et al. (1987) line. Results from this study supporting this claim are given below.

Along strike changes in margin morphology. Figure 2.7 compares four lines that include from east to west: Line 22 off the northwest coast of Puerto Rico, Line 6 off the east-central coast of Puerto Rico in the area of the Toa Baja well and Line 2 of Larue and Berrong (1991), Line 9 off of eastern Puerto Rico, and Line 14 off the Virgin Islands shelf. Enlargements of critical areas on these lines are provided in Figure 2.8.

The margin exhibits progressive erosion and collapse from west to east. In the east the margin appears to represent a complete section including a 70 m thick cap of early Pliocene Quebradillas limestone. The total thickness of the margin is about 1 km. Heezen et al. (1985) report a 1200 m thickness of the carbonate margin overlying Eocene metavolcanic rocks based on their Alvin dives in the east wall of the Mona Canyon.

On Line 14 near the Virgin Islands platform, south-dipping reflectors are similar to those imaged and drilled by Larue and Berrong (1991) on Line 2 and in the Toa Baja well (Figs. 2.6 and 2.7). This suggests that the carbonate platform has been reduced erosion or slumping to a thickness as small as about 0.5 km.

Margin morphology compared to predictive models. The preferred model on beginning this study was that the Puerto Rico trench formed by the collision of an obliquely subducting Atlantic fracture zone. Elaborating on the tectonic erosion hypothesis of Birch (1986), Dolan and Wald (1994) proposed that the 4 km of late Neogene subsidence and the reentrant in the northern Puerto Rico slope occurred in response to removal of topographic support for the Puerto Rico shelf provided by underthrusting fracture zones and overlying carbonate banks as the

colliding ridges swept westward through time. This model would predict localized and time transgressive subsidence tied to specific fracture zones and the southeastern extension of the Bahama platform.

More detailed correlations between closer spaced SCS lines from EW96-05 are needed to test this idea of diachronous deformation along the margin. It is clear that deformation did not involve any post-middle Oligocene (San Sebastian Formation) compressive deformation of the carbonate cap (Figs. 2.6 and 2.7) and that the cap subsided at a uniform rate that resulted in a uniform along-strike northward dip of about 4° (Moussa et al., 1987; Birch, 1986).

Barrier reef complex. The existence of a barrier reef complex well imaged on Line 9 and suggested on Lines 22 and 6 (Fig. 2.8) is proposed here for the first time based on these SCS data. Because the reef appears to plunge to greater depths (or at least be less exhumed) in northwest and east-central Puerto Rico, previous studies in this area may have confused its constructional profile and reflection-free character with underlying Eocene arc basement (Larue and Berrong, 1991). In the less well studied western area for which we have seen no previous seismic data, the top of the reef lies within 0.5 seconds of the seafloor. Line 9 reveals that the reef complex is bounded to the south by a recently active fault exhibiting a "flower structure" of possible strike-slip origin. Down-to-the-south motion on this fault may have created a high upon which initial reef growth occurred. Detailed correlation between these sections and the Toa Baja and CPR-4 wells is needed to confirm the age of reef growth and drowning as well as its along strike continuity. Assuming the reef formed as a continuous barrier-type reef along the north coast, its drowning may be also related to the northward tilting of the Puerto Rico shelf that caused it to subside at a greater rate than could be matched by its upward growth. Reef growth may correlate with several Oligocene-Pliocene transgressive-regressive cycles outlined by Seiglie and Moussa (1985).

Other Hypotheses Addressed During This Study

1. Uplift mechanism for the Mona block and the Aguadilla arch of northwest Puerto Rico: An effect of oblique subduction of the southeastern end of the Bahama platform or restraining bend tectonics? Dolan and Wald (in press) propose that the Mona Block may be the surface expression of the subducted southeastern margin of the Bahama platform. Dredge hauls indicate that the Mona block is composed of blueschist rocks of Cretaceous age and similar to those exposed on the Samana Peninsula of the eastern Dominican Republic. This uplift mechanism is similar to that proposed by McCann and Sykes (1984) for the uplift of the Main Ridge. The topographic effects of such a model could also be explored for the Quaternary uplift of the island of Puerto Rico. Gardner et al. (1981) point out the highest Quaternary shoreline features are located on the Aguadilla Peninsula which is on the landward projection of the Mona block high.

An alternative model is that the Mona block is uplifted at a gentle restraining bend formed along the west-northwesterly striking Septentrional fault zone. The eastern limit of the bend is marked by the abrupt transition from EW to ENE-striking strike-slip faults to WNW faults in the Mona Canyon area. This bend similar in dimensions, style, and bedrock geology to the gentle bend exposing rocks of the Samana Peninsula. The occurrence of localized folding at the base of the Mona block in turbidites of the Puerto Rico trench may also be explained by a bend in this area. Evaluation of this model awaits the availability of processed MR1 sidescan and bathymetric data from this complex area.

2. Tectonic origin of the Mona Canyon and Mona Passage extensional zone and its relationship to Caribbean-North America strike-slip faults Speed and Larue (1991) argue that late Neogene extension in a north-south direction affected Puerto Rico, the Puerto Rico trench, the Mona Passage, and the Anegada Passage. The main zone of extensional detachment was

assumed to be a south-dipping Puerto Rico trench. The hanging wall was assumed to be the drowned island slope of Puerto Rico largely on the basis of its slight anticlinal arching.

MR1 sidescan data from the Mona Passage support the idea of regional extension but in an east-west rather than north-south direction. X-shaped conjugate fault pairs affecting the submerged early Pliocene carbonate cap. The orientation of these fault pairs is particularly well expressed in the area west and southwest of Mona Canyon indicate post-Early Pliocene? extension in an east-west direction. The northwest-striking fault in this pair are thought to be right-lateral oblique-slip faults while the northeast fault is assumed to be a left-lateral oblique-slip fault. North-south-trending rifts such as the Mona Canyon and the Yuma basin are also present and drop the carbonate platform down to depths of 1 km in full and half grabens beneath the adjacent seafloor (Figs. 2.9 A, B, C and D). Diffuse extension probably forms the western margin of the Puerto Rico microplate first postulated by Byrne et al. (1987). GPS studies support such a model because the rate of eastward motion of the Puerto Rico microplate is twice that of the adjacent microplate in Hispaniola (Farina et al., 1995). The interplay between north-south rifts like the Mona Canyon and the east-west striking Septentrional fault zone is complex and will require detailed study.

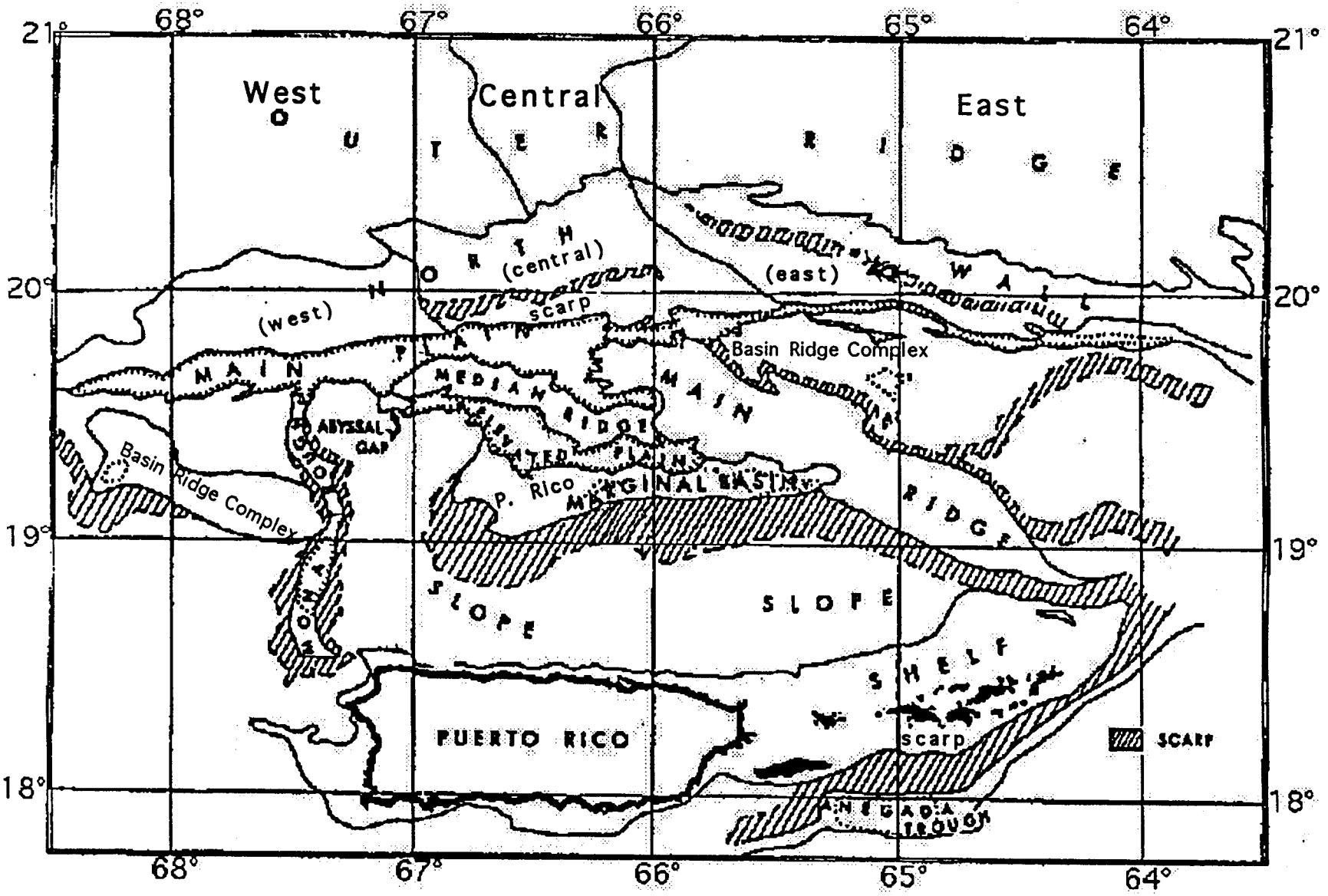

Figure2.1 General physiography and geomorphological features of the Puerto Rico Trench (Modified from Ewing, Lonardi, and Ewing et al. 1966).

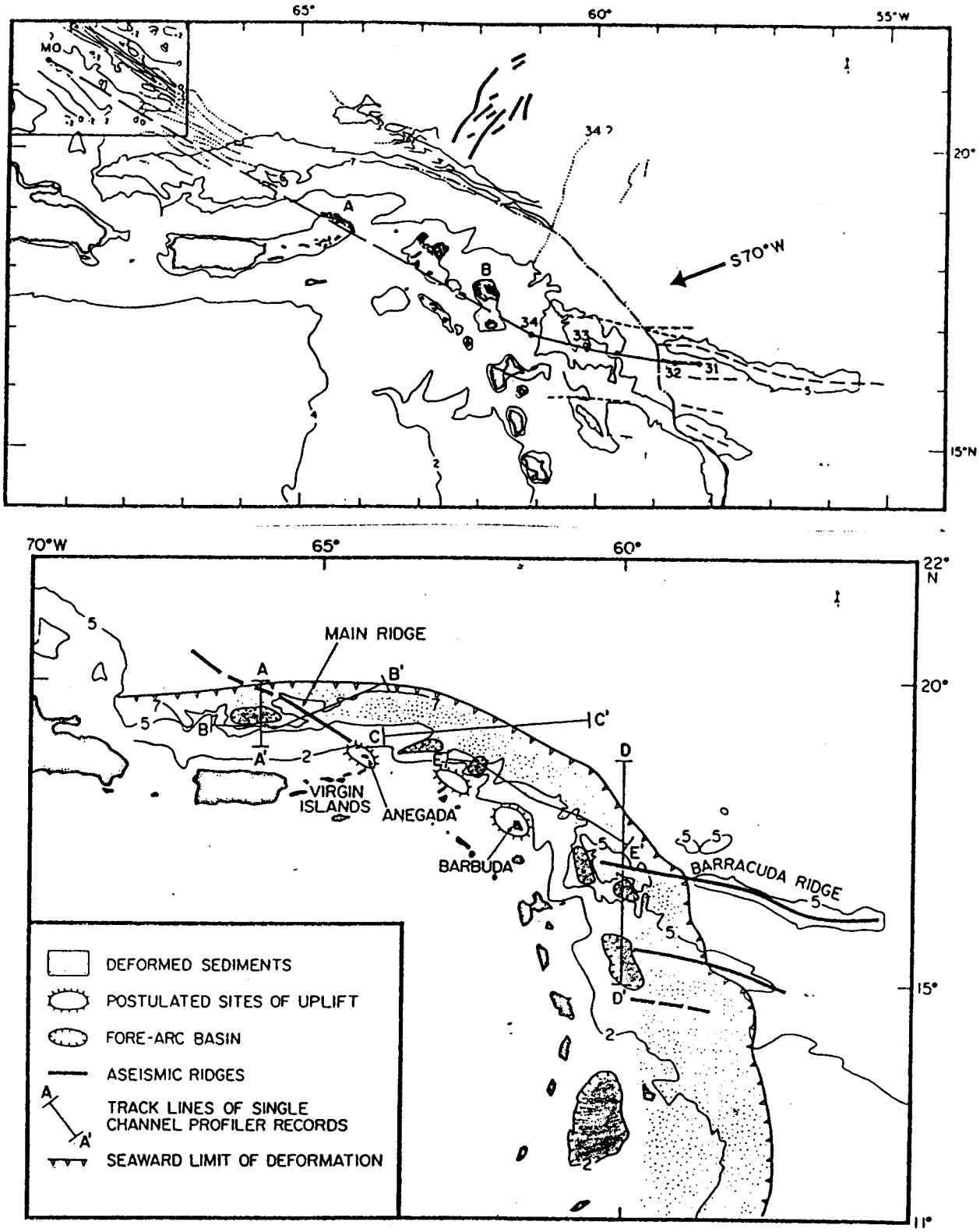

Figure 2.2A. Fracture zone and oceanic spreading fabric at the northeastern margin of the Caribbean plate from McCann and Sykes (1984). The dashed line shows the postulated extent of the subducted Main Ridge-Barracuda Ridge beneath the Caribbean plate. **B.** Geologic effects of the subduction of the Barracuda-Main Ridge according to McCann and Sykes (1984). Note the presence of a semi-continuous "classic" forearc basin along the leading edge of the Caribbean plate. A-A′ and B-B′ give the locations of seismic lines shown in Figure 2.

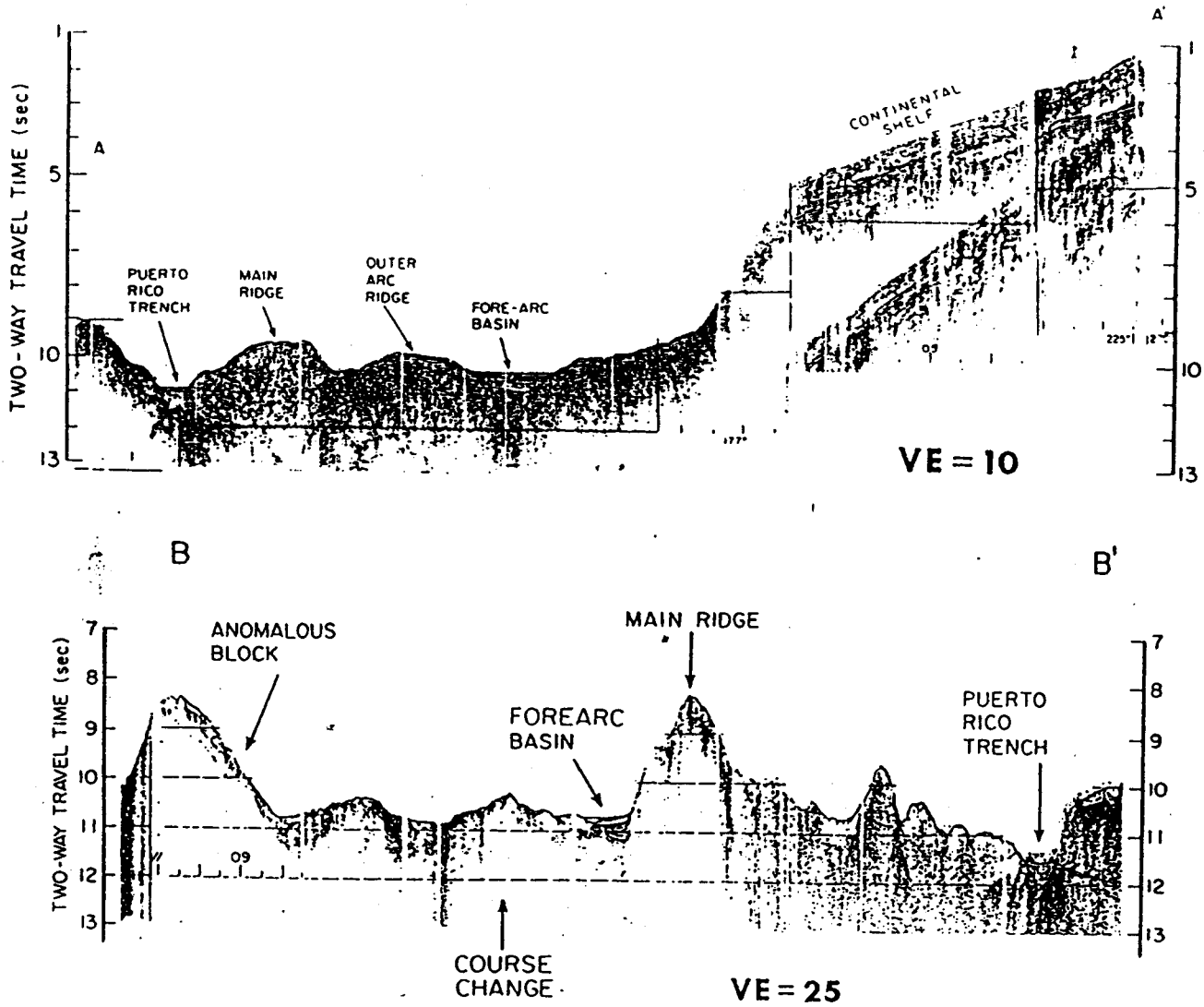

Figure 2.3A. Line A-A′ from McCann and Sykes (1984) in the EW96-05 survey area. See text for discussion. **B.** Line B-B′ from McCann and Sykes (1984) east of the EW96-05 survey area. See text for discussion.

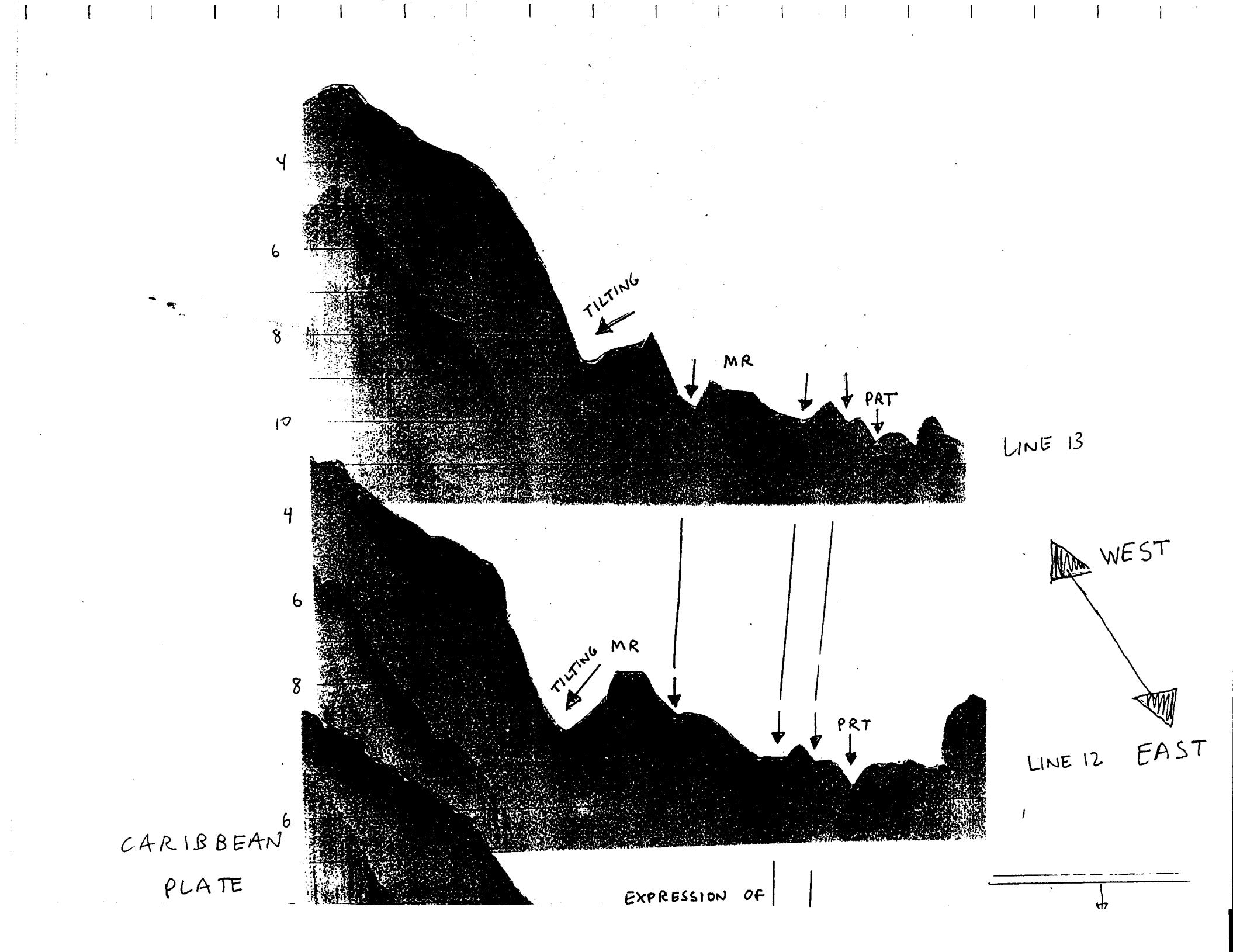
4
6
8
10
TILTING
MR
PRT
LINE 13
4
6
8
6
TILTING
MR
PRT
WEST
LINE 12
EAST
CARIBBEAN
PLATE
EXPRESSION OF

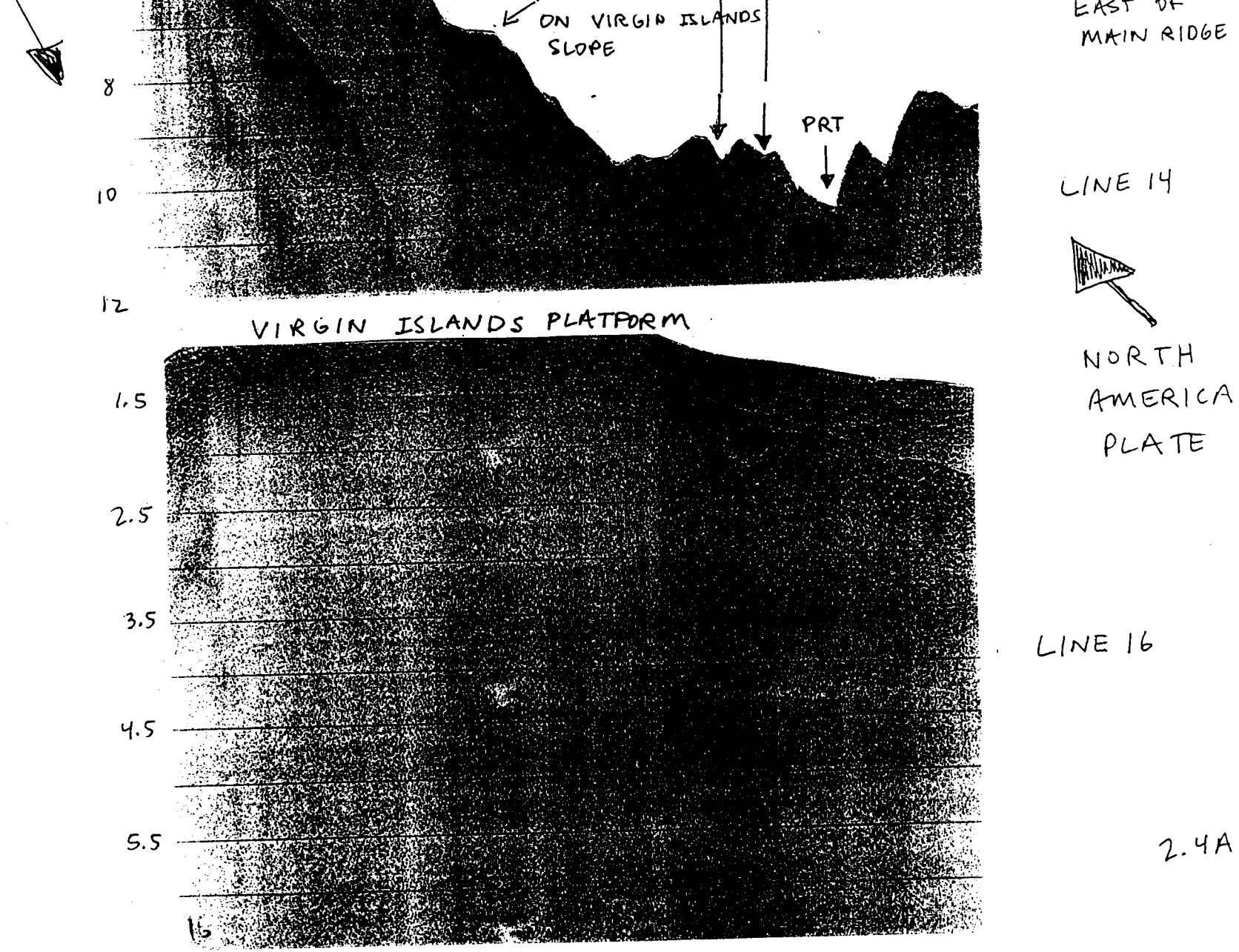

Figure 2.4A. Unmigrated SCS profiles processed by J. P. van Gestel using SIOSEIS from the eastern part of the EW96-05 study area. Lines indicate proposed correlations of ridges and faults along their strike. B. Profiles from the central part of the study area. C. Profiles from the western part of the study area.

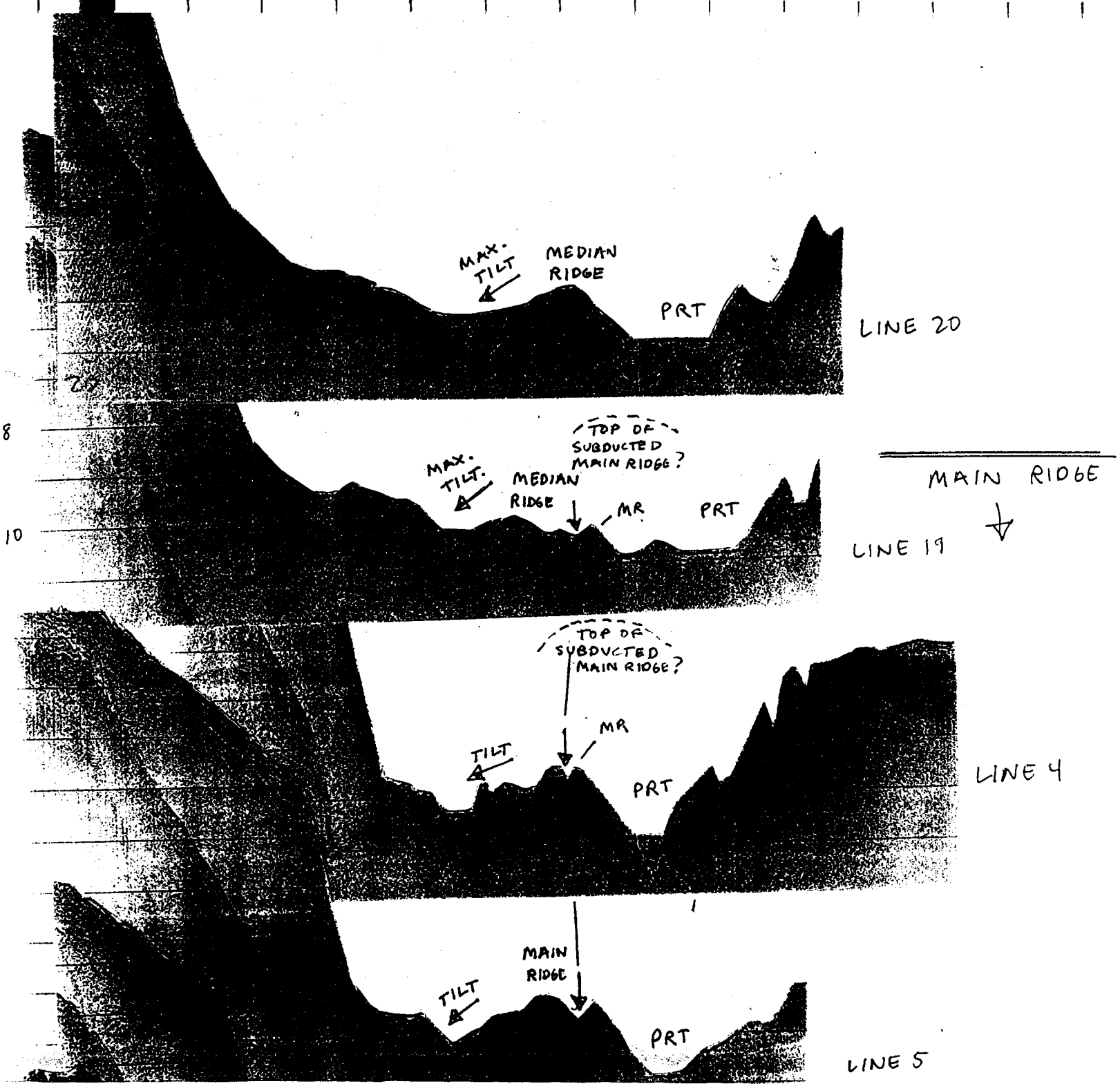
MAX. TILT
MEDIAN RIDGE
PRT
LINE 20
TOP OF SUBDUCTED MAIN RIDGE?
MAX. TILT.
MEDIAN RIDGE
MR
PRT
LINE 19
MAIN RIDGE
TOP OF SUBDUCTED MAIN RIDGE?
MR
TILT
PRT
LINE 4
MAIN RIDGE
TILT
PRT
LINE 5

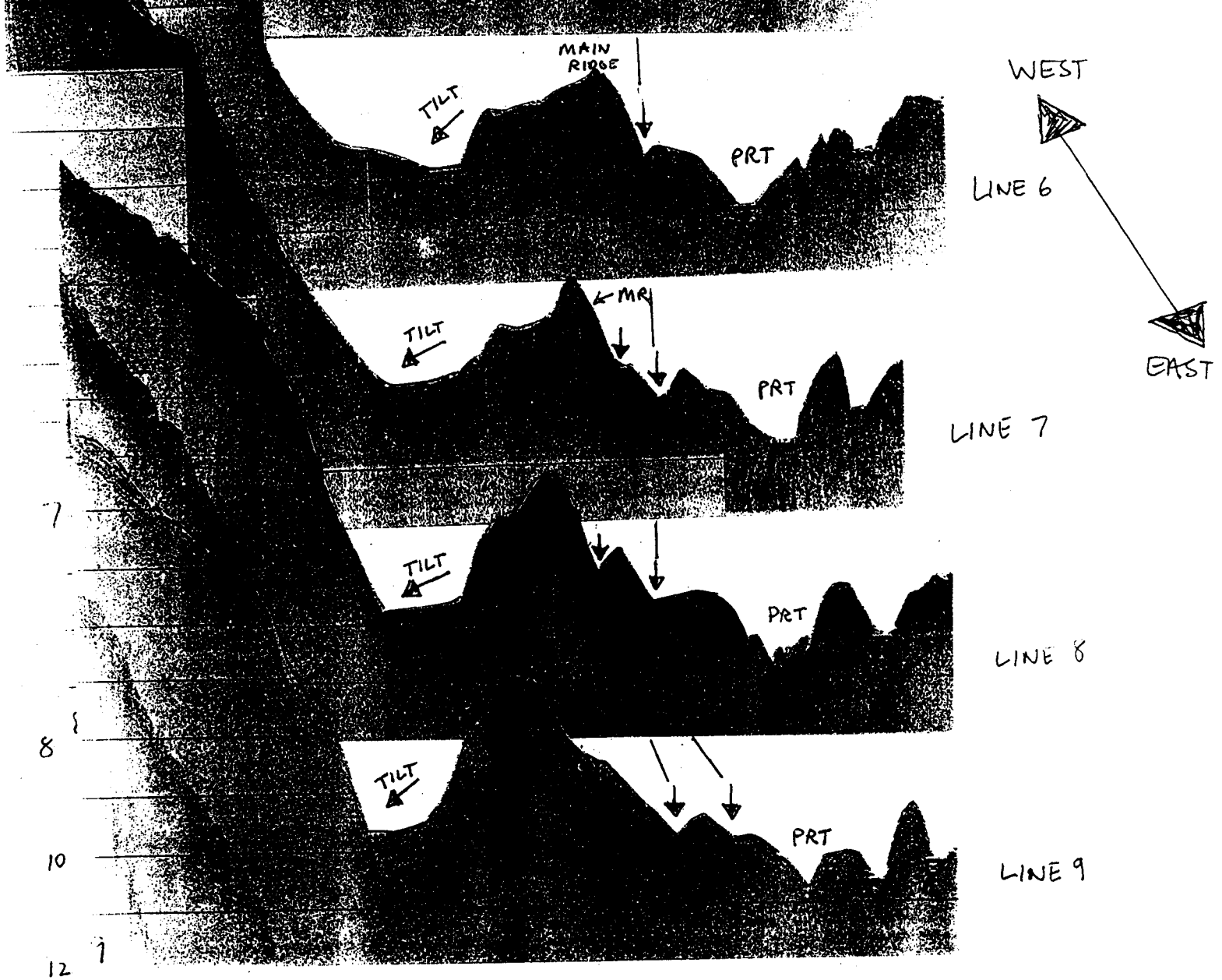
MAIN RIDGE
TILT
PRT
LINE 6
WEST
EAST
MR
TILT
PRT
LINE 7
TILT
PRT
LINE 8
TILT
PRT
LINE 9
7
8
10
12

2.4B

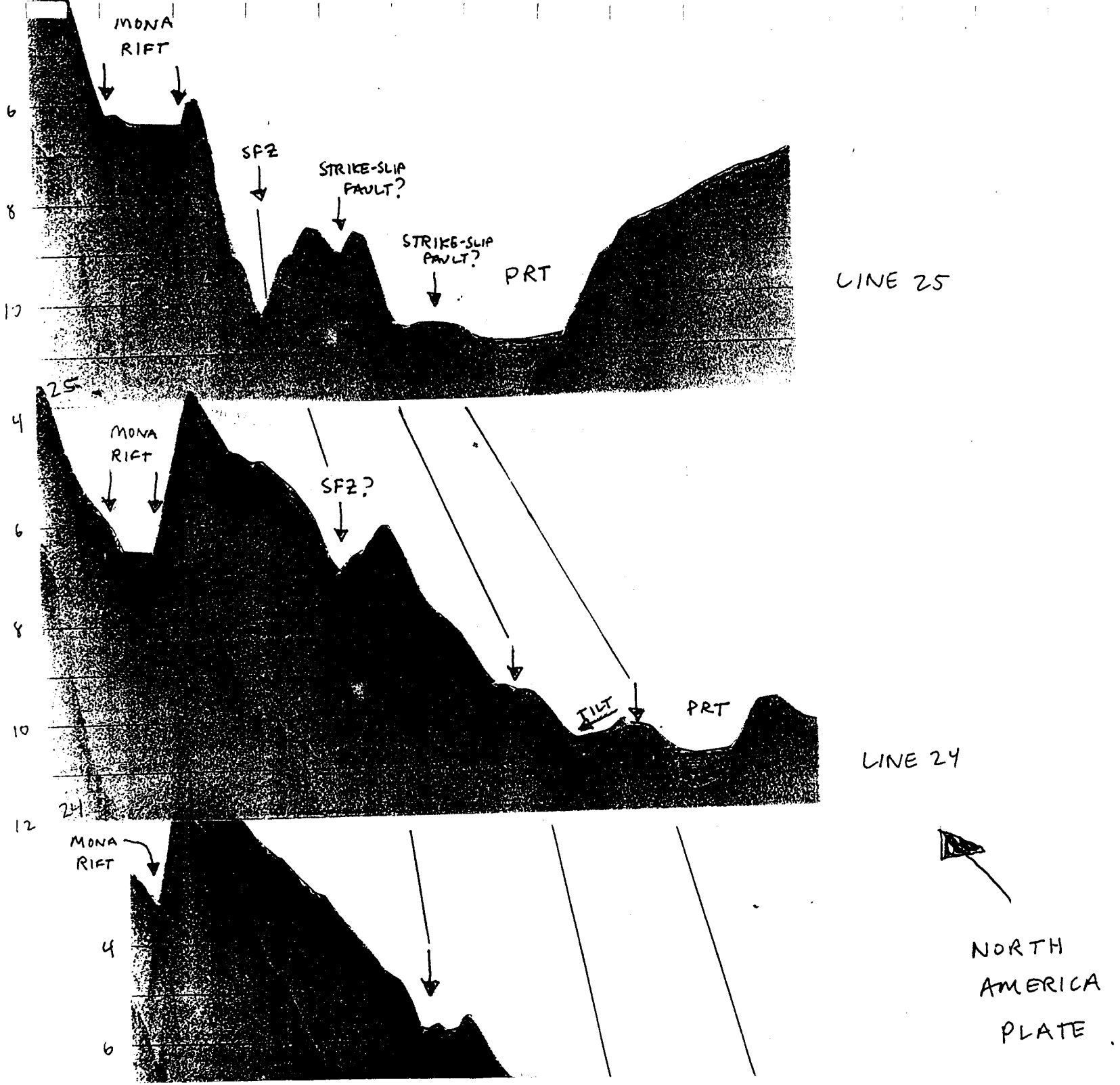
MONA RIFT
SFZ
STRIKE-SLIP FAULT?
STRIKE-SLIP FAULT?
PRT
LINE 25
MONA RIFT
SFZ?
TILT
PRT
LINE 24
MONA RIFT
NORTH AMERICA PLATE

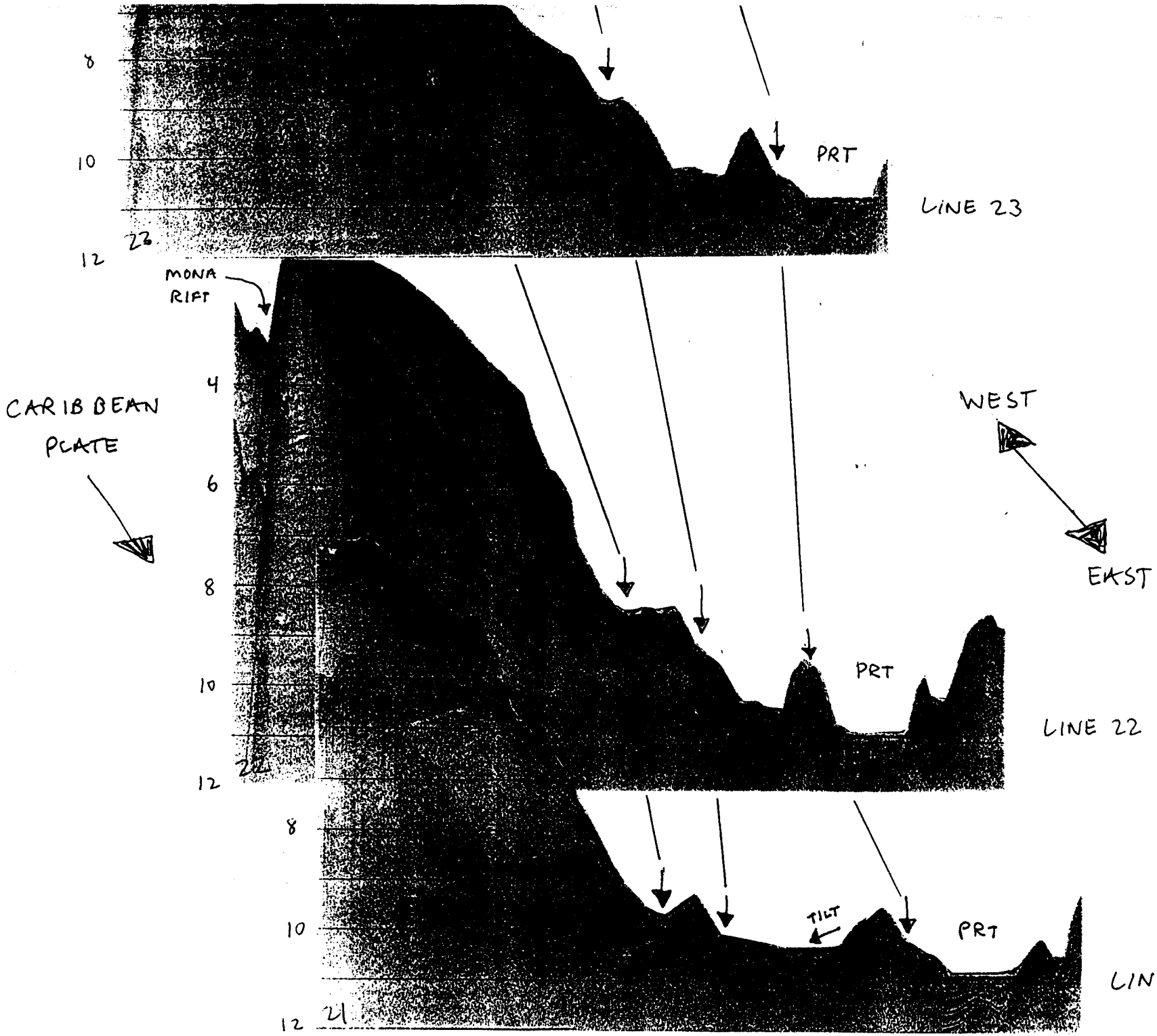
8
10
12
23
PRT
LINE 23
MONA
RIFT
CARIBBEAN
PLATE
4
6
8
10
12
22
WEST
EAST
PRT
LINE 22
8
10
12
21
TILT
PRT
LINE 21

2.4C

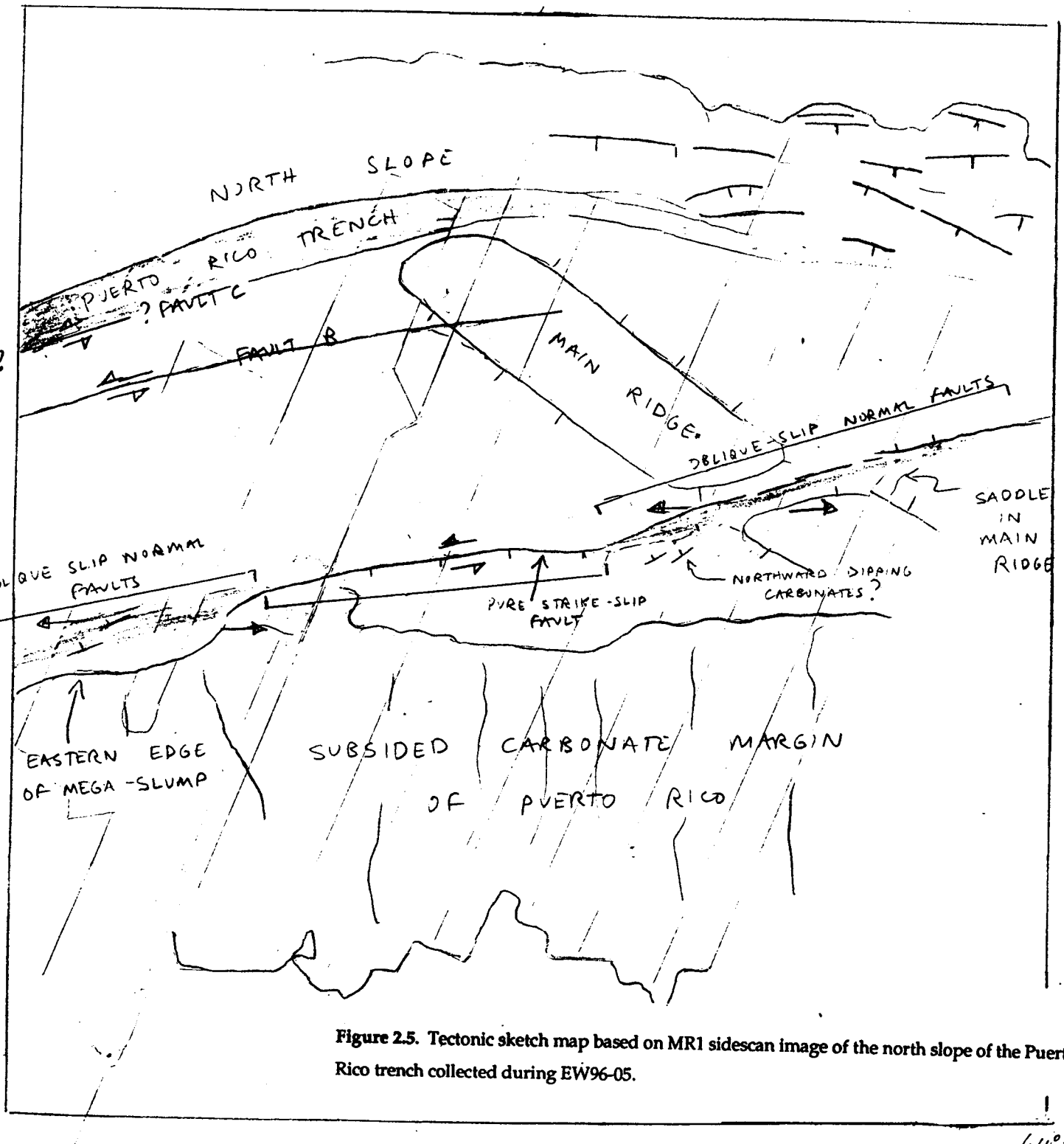

Figure 2.5. Tectonic sketch map based on MR1 sidescan image of the north slope of the Puerto Rico trench collected during EW96-05.

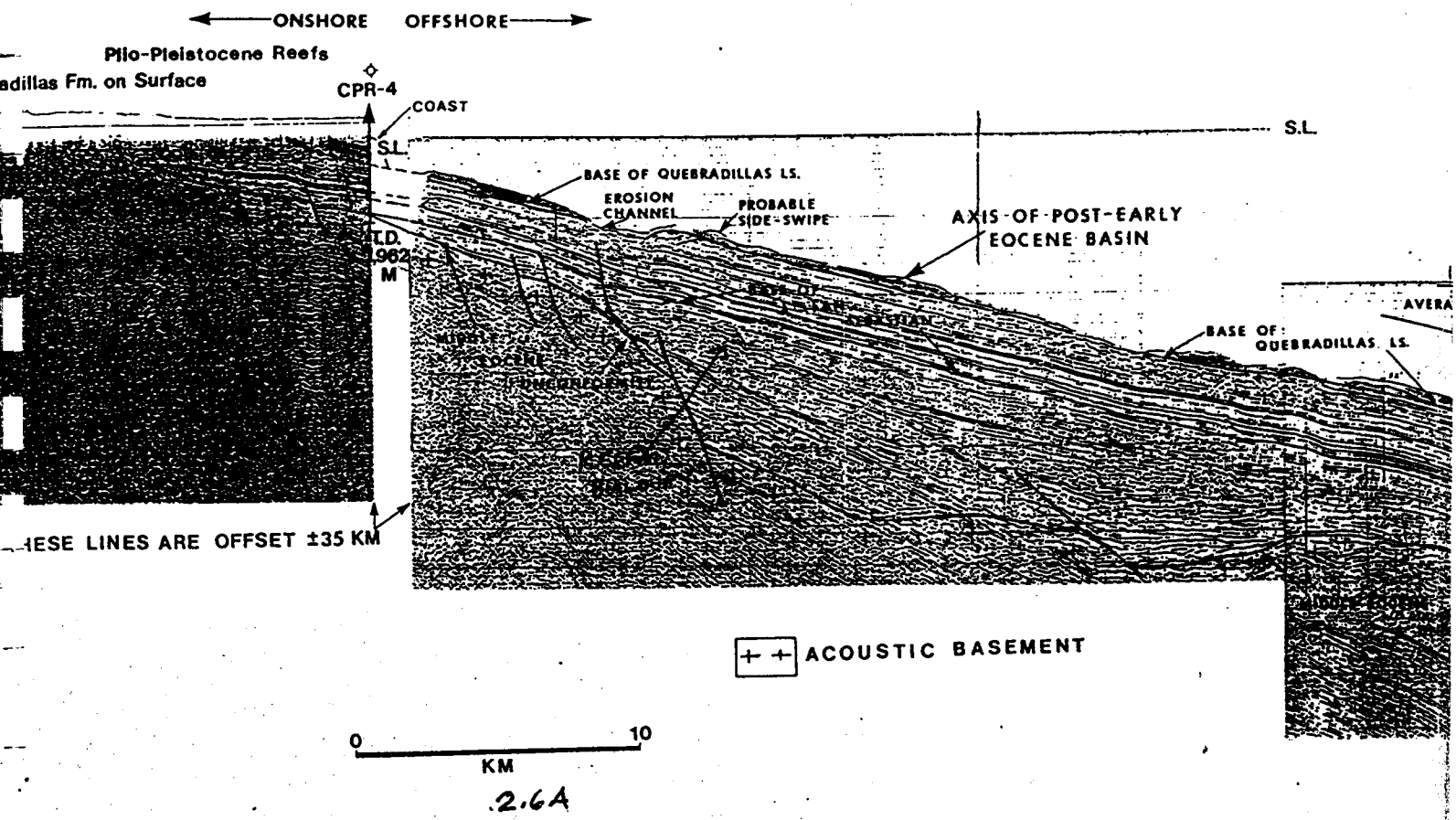

2.6A

Figure — South-north 1200% CDP seismic line T-111D (Western Geophysical Company), North Coast (Arecibo) Tertiary basin. The bottom of the Puerto Rico Trench is just off the line at the right. The 4CPR well is shown at the left end of the line. The Quebradillas Limestone forms a discontinuous veneer at the top of the section to ~5,200 m water depth. Seismic interpretation is by E. A. Krieg; geologic interpretation is by A. A. Meyerhoff and I. Taner. From Alonso and others (1987). Location of the line is shown in Figure 12.

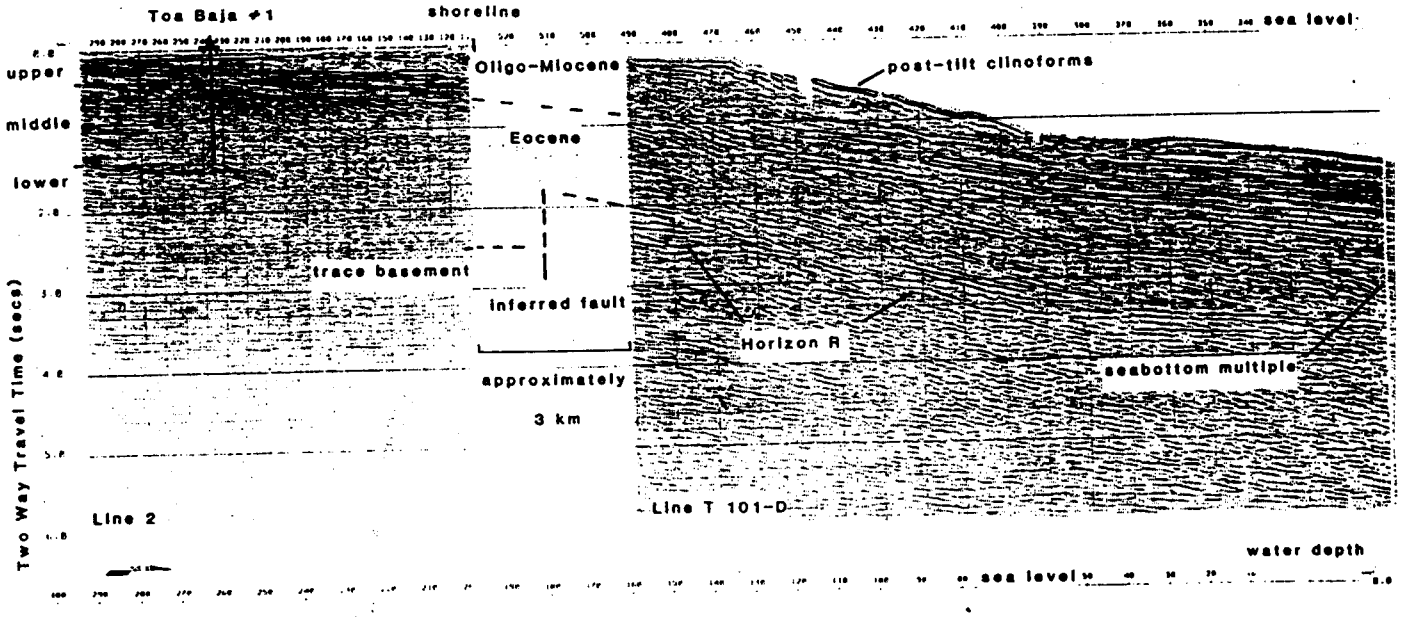

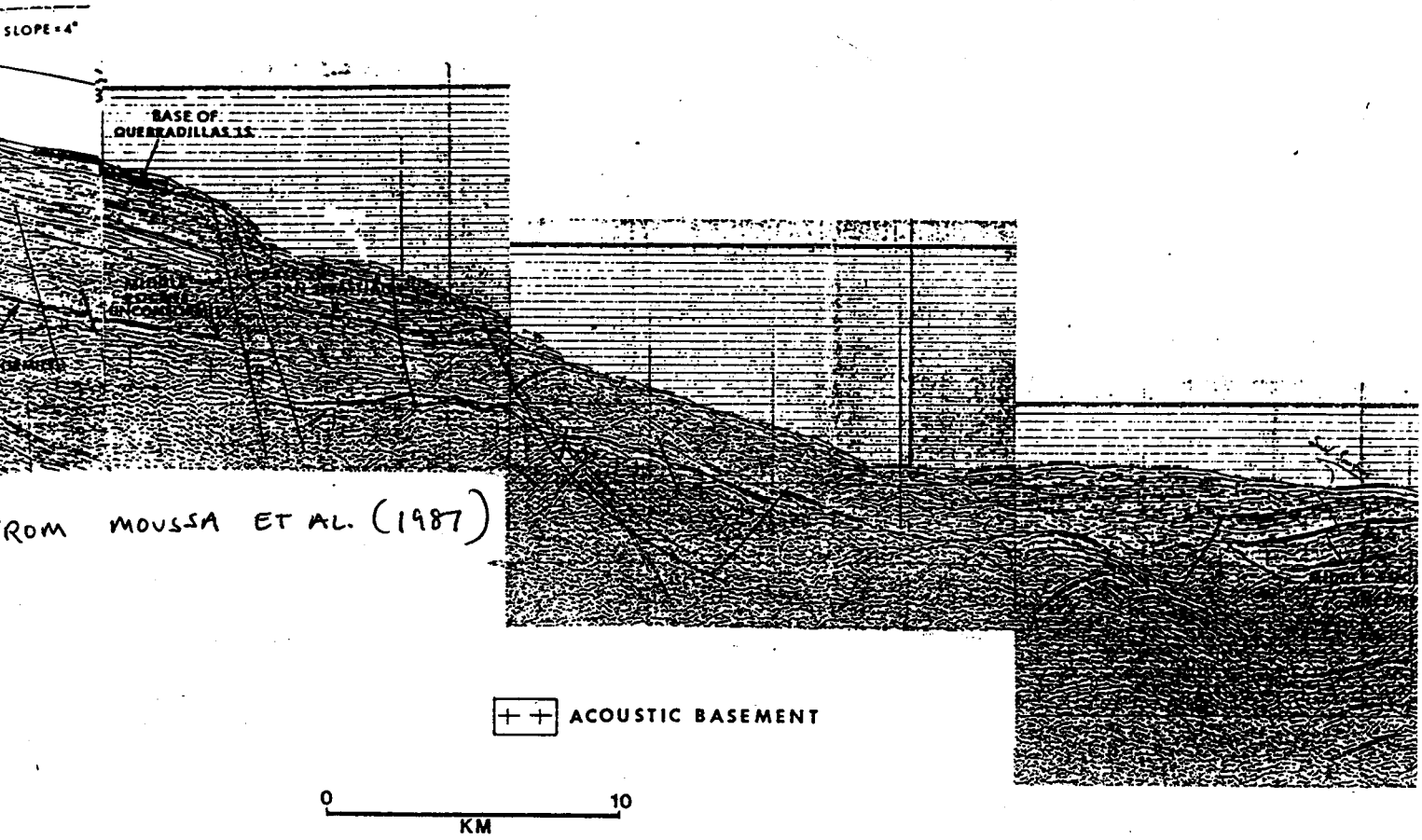

FROM MOUSSA ET AL. (1987)

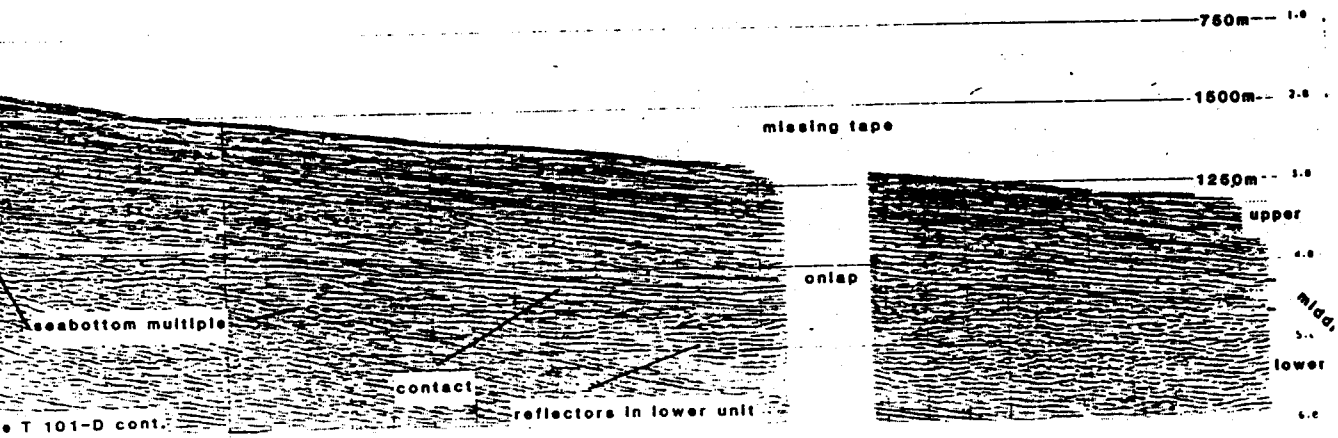

FROM LARUE AND BERRONG (1991)

2.6B

Fig Seismic reflection Line 2 and T101-D, located in Figure 1. Both lines shot by Western Geophysical, Inc. Line 2 is 120 channel, line T101-D is 24 channel. Processed by Berrong Enterprises, Ltd using no automatic gain correction (true amplitude reflectors). For scale, length of Line 2 is approximately 7'km. On Line 2, "trace basement" is from cross-line. Low angle discordances in Line 2 middle unit near drillsite probably thrust faults. Change in depth to basement from Line 2 to Line T 101-D thought to be a product of a pre-Oligocene fault. Post-tilt clinoforms probably Late Miocene to Pleistocene in age. Onlap near SP 100, Line T 101-D is from dip-correcting downlap using Oligocene-Miocene reflectors as horizontal datum. Depth of Toa Baja well was 2.704 km.

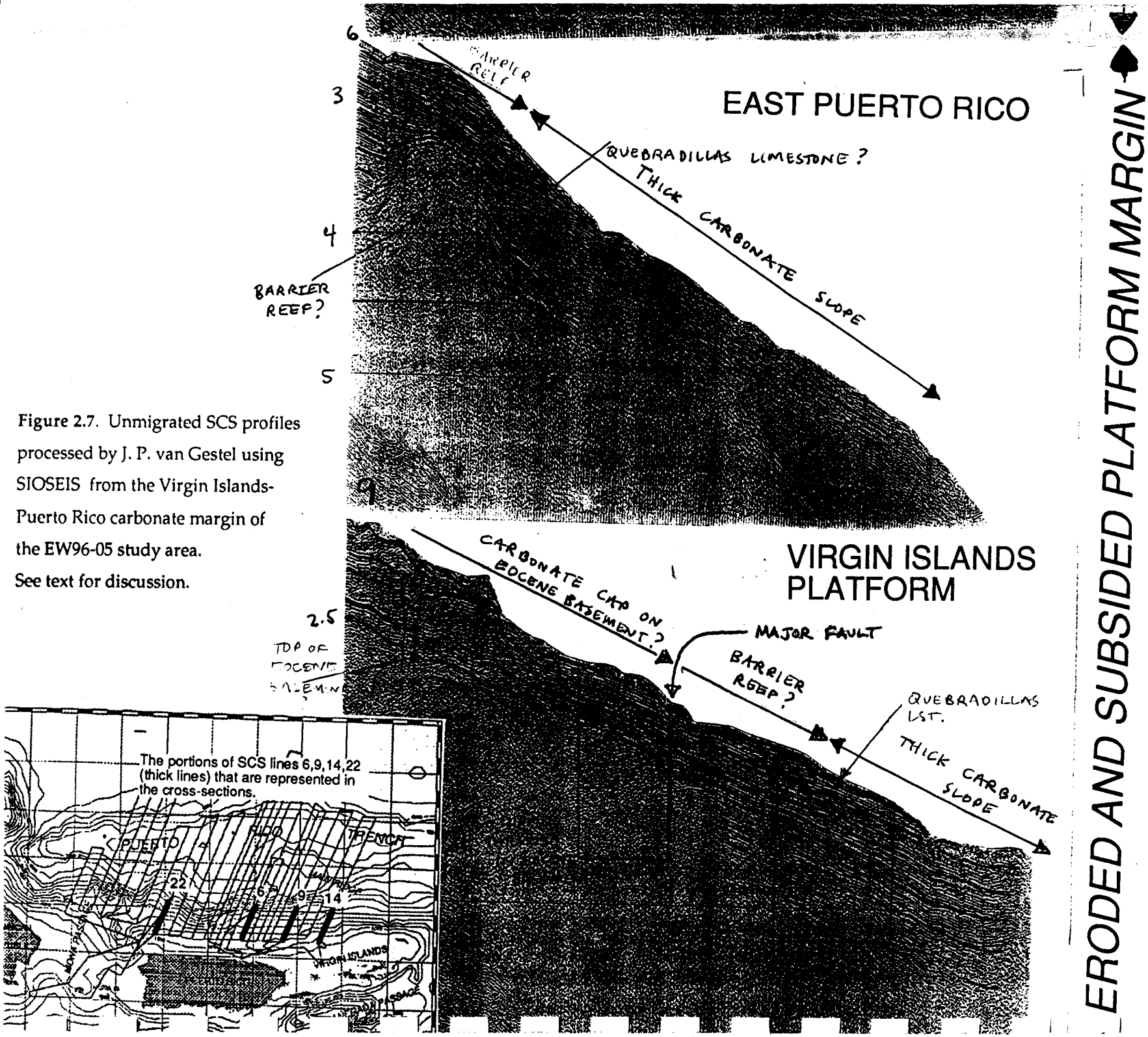

Figure 2.7. Unmigrated SCS profiles processed by J. P. van Gestel using SIOSEIS from the Virgin Islands-Puerto Rico carbonate margin of the EW96-05 study area. See text for discussion.

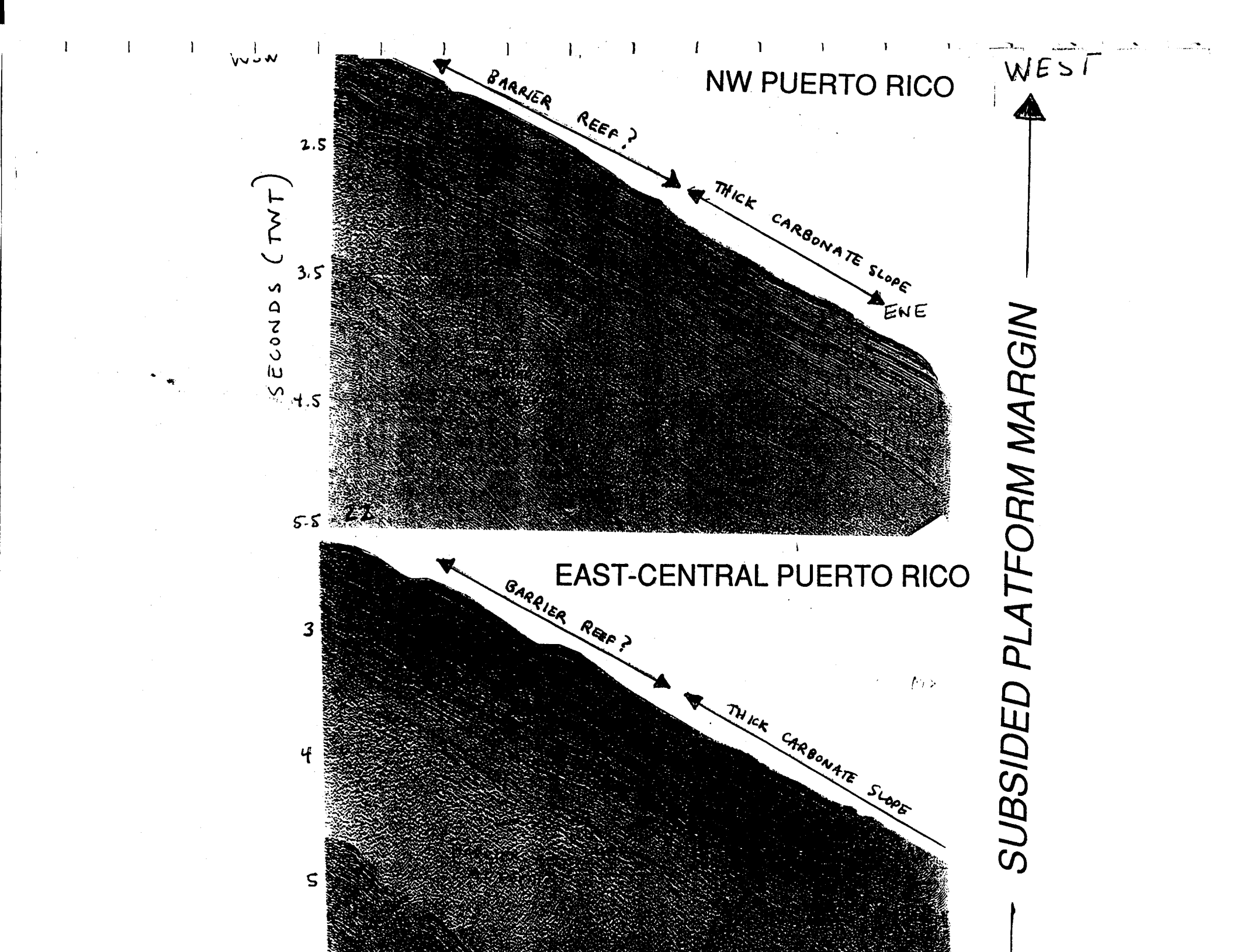
WSW
NW PUERTO RICO
BARRIER REEF?
THICK CARBONATE SLOPE
ENE
SECONDS (TWT)
2.5
3.5
4.5
5.5
EAST-CENTRAL PUERTO RICO
BARRIER REEF?
THICK CARBONATE SLOPE
3
4
5
WEST
SUBSIDED PLATFORM MARGIN

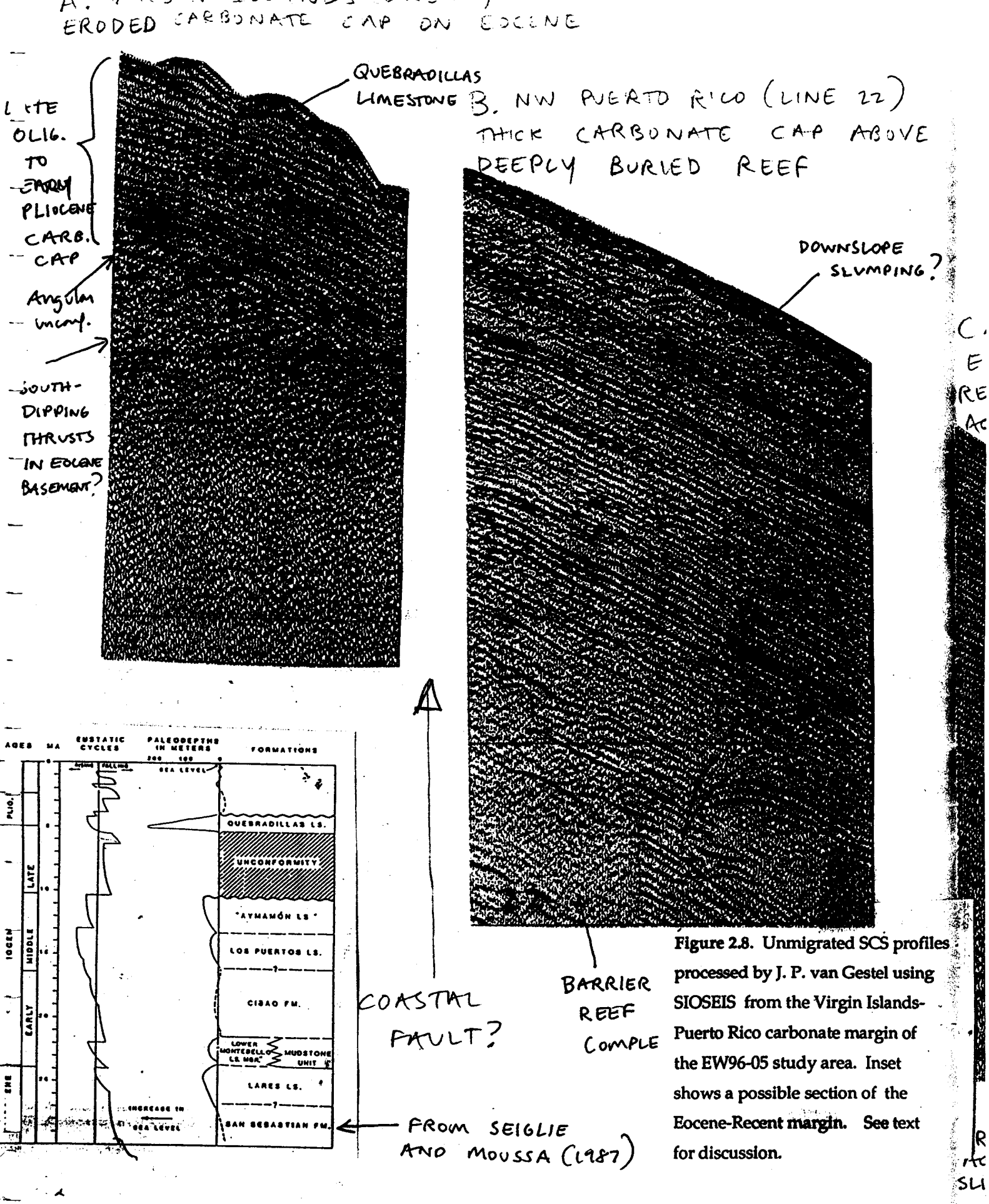

Figure 2.8. Unmigrated SCS profiles processed by J. P. van Gestel using SIOSEIS from the Virgin Islands-Puerto Rico carbonate margin of the EW96-05 study area. Inset shows a possible section of the Eocene-Recent margin. See text for discussion.

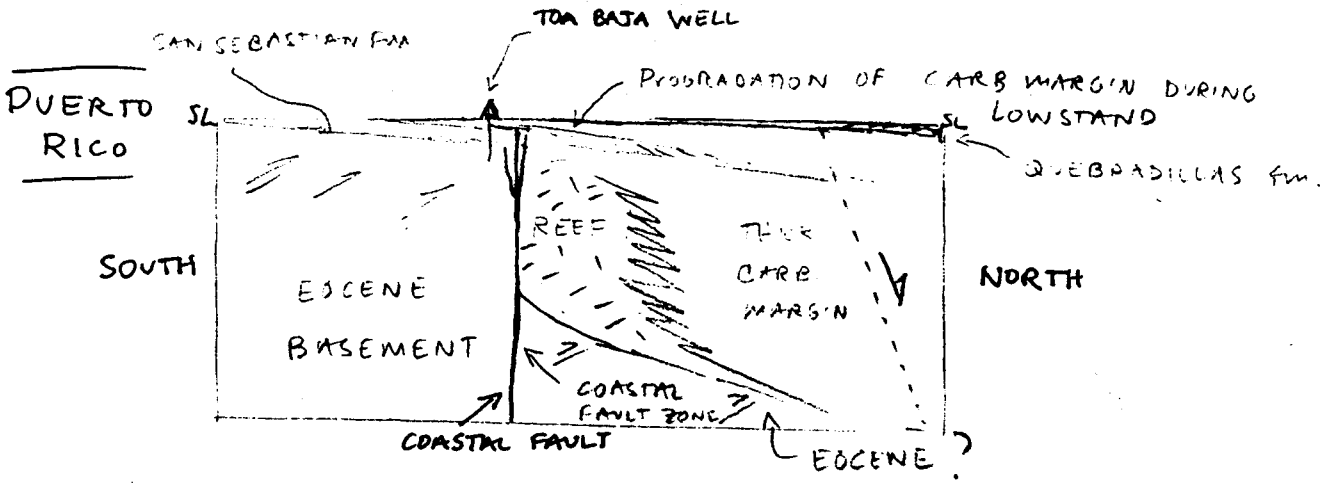

EAST PUERTO RICO (LINE 9)

ODED CARBONATE CAP ABOVE EXHUMED
F ; COASTAL FAULT RECENTLY
TIVE

D. VIRGIN ISLANDS (LINE 14)

ERODED CARBONATE CAP ABOVE REEF ; PROGRADATION O CARBONATE MARGIN DURING LOWSTAND

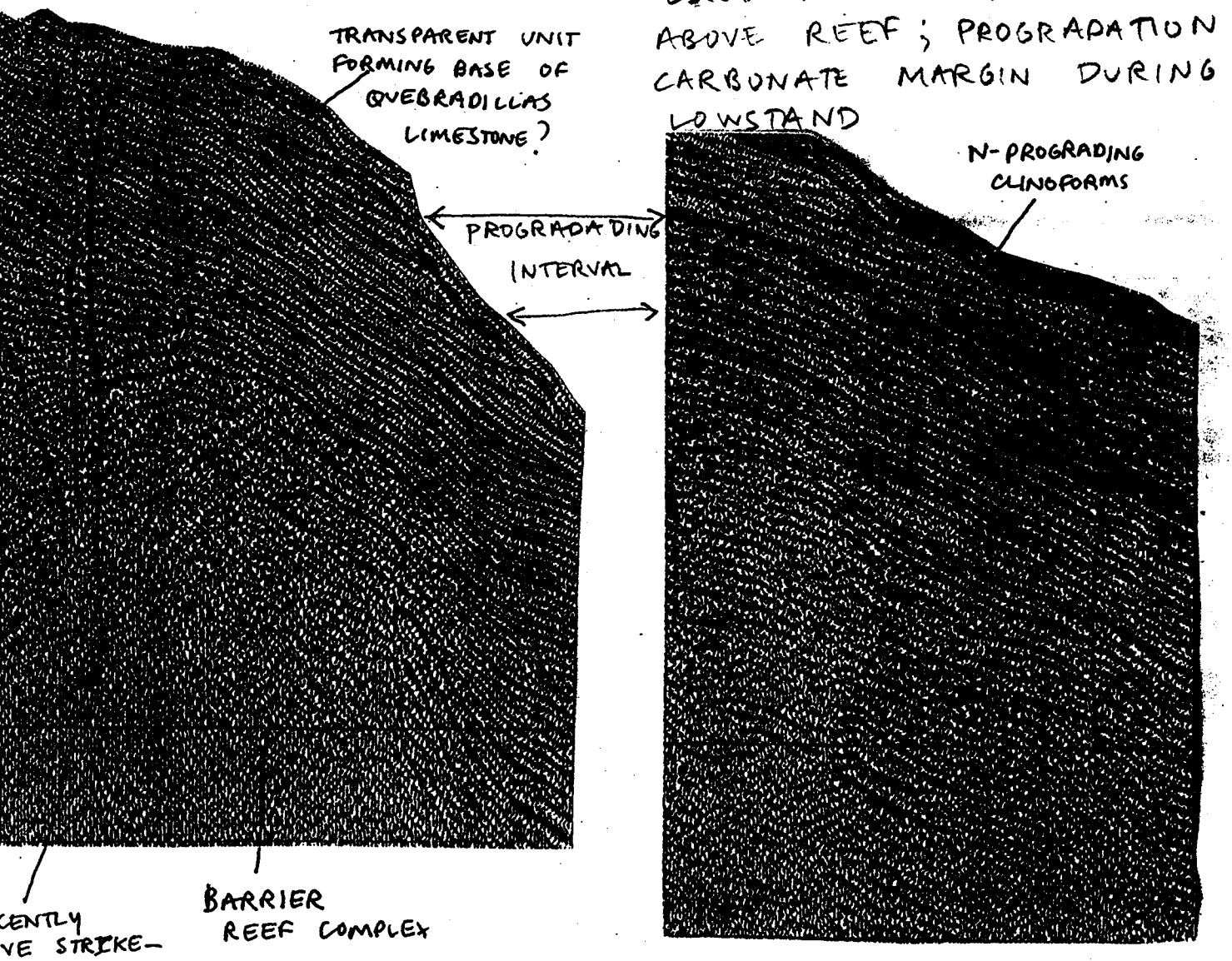

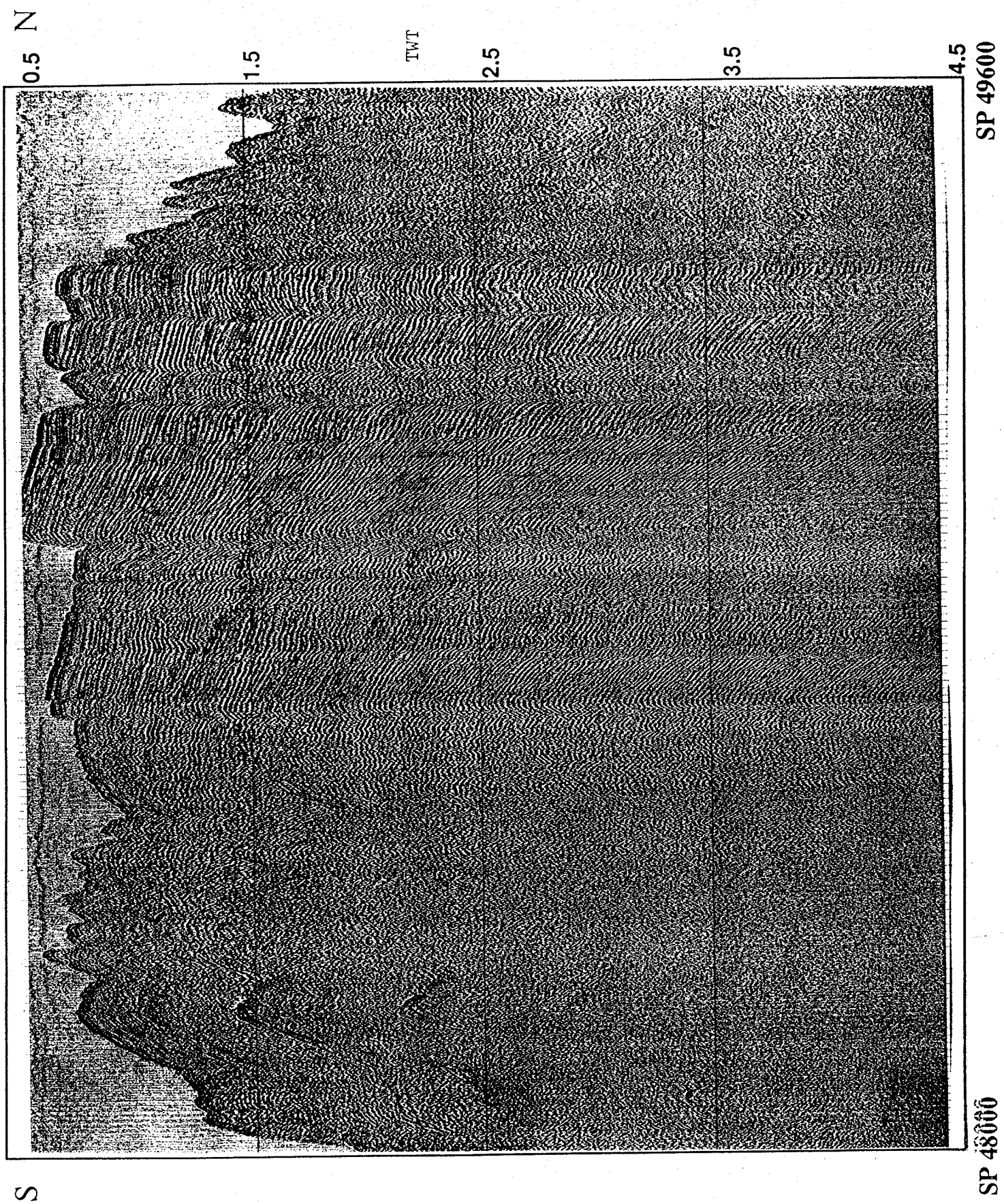

Figure 2.9 Line 35 Mona Passage.

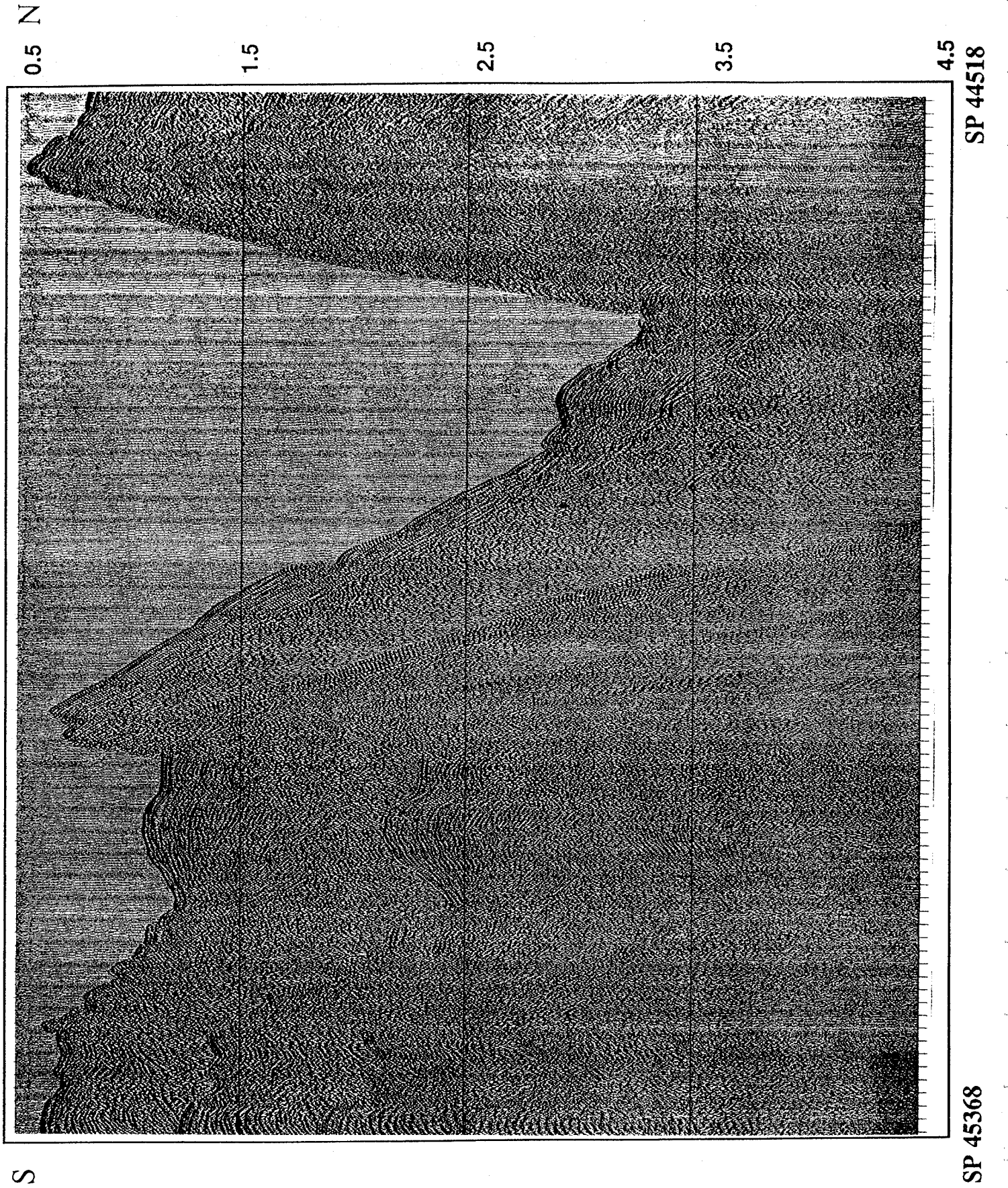

Figure 2.9B: Line 32 Desecheo Ridge.

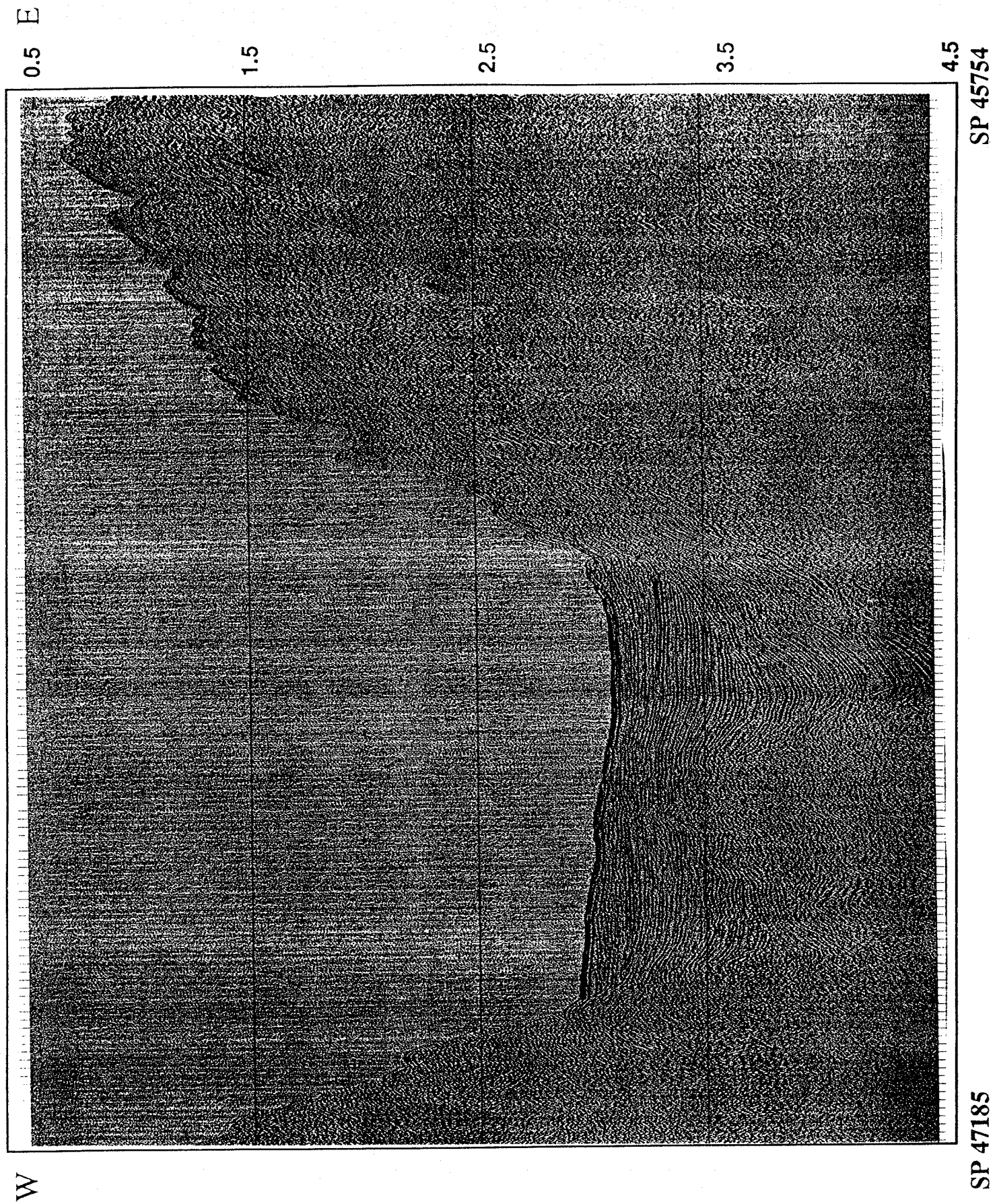

Figure 2.9c: Line 34 Yuma Basin.

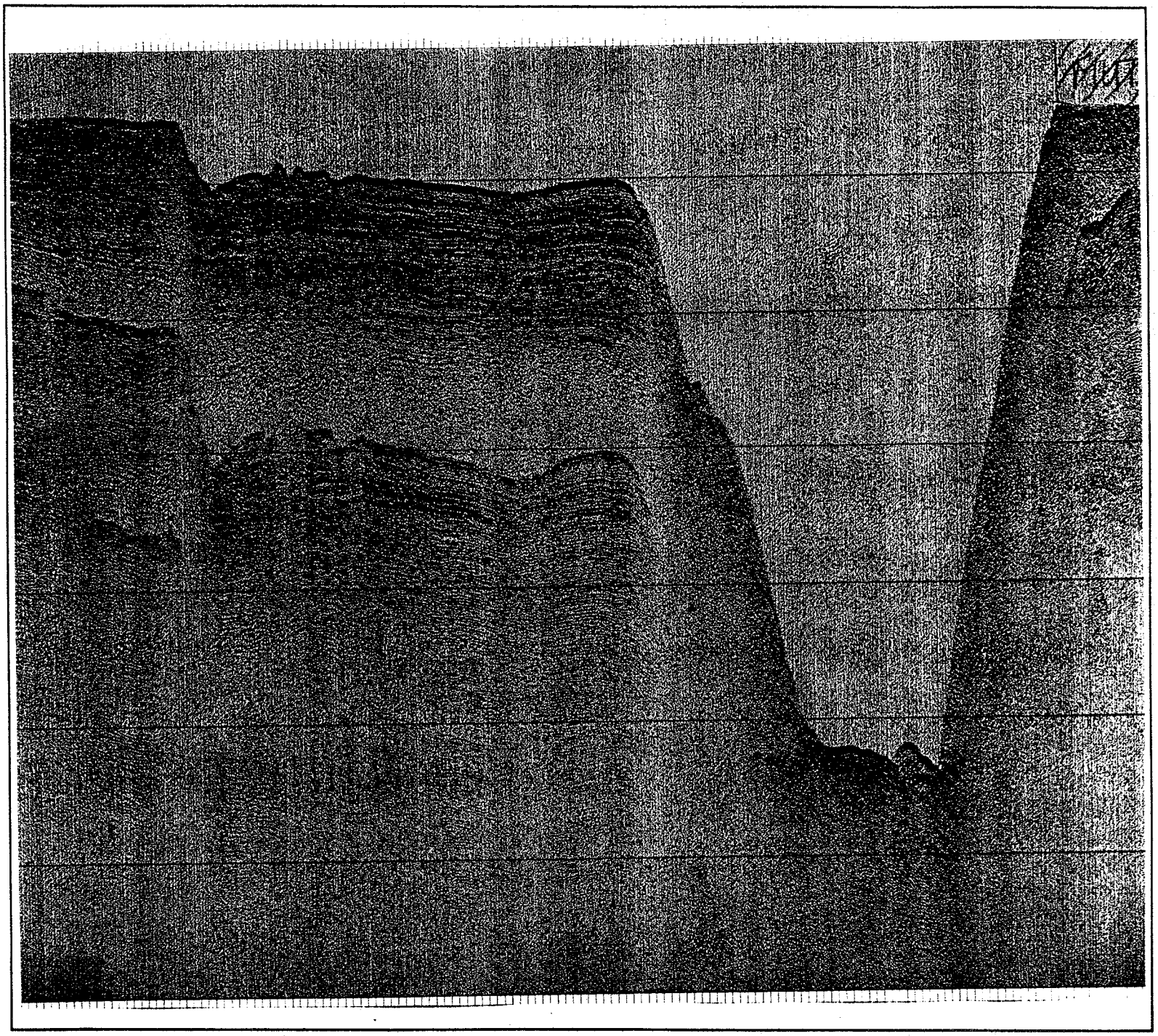

Figure 2.9D Line 31 Mona Canyon.

CHAPTER 3. SINGLE-CHANNEL SEISMIC REFLECTION OPERATIONS

by Jean-Paul van Gestel

Streamer

The "Single-Channel Streamer" (SCS) is a multi-channel streamer that usually consists of 4 to 8 channels (Figs. 3.1 & 3.2). During the EW96-05 cruise, only four of the channels were utilized. The SCS preamplifier is can handle up to 8 channels of data. Streamer had carried the preamplifier itself up until around 1988, and had provided both amplification and a low impedance, single ended output. After this time, commercially built transformer-coupled streamers introduced the problem of having to deal with low-impedance, low-level, differential signal. This problem was overcome with the building of a transformer-coupled preamplifier by Harry Van Santford. This preamplifier provides amplification of the streamer channels for digitization purposes and allows the merging of the individual channels into one channel. This in turn allows the data to be displayed on the line-scan recorders.

The differential analog signal from each of the steamer channels is amplified and converted to a single-ended signal by the transformer-coupled amplifier. The signals are then sent to a 4-channel digitizer and to the buffer-amplifiers. The buffer-amplifiers then send their signal to the front panel (which is kept in the wet-staging area) on the as a test and then to the 8-channel adder. The adder permits any of the channels to be combined to form a single analog signal. This single analog signal is then sent through a variable-gain amplifier and then to the line scan recorders. The gain of the variable-gain amplifier is usually set at 10 dB while the total gain at the preamplifier is around 70 dB.

The streamer used during this cruise consisted of 7 components. They will be described in order from the fantail of the ship to the end of the streamer. The first component was the 156.75 m kevlar tow leader. The next is a 25 m stretch section followed by a 25 m non-stretch rope. After this there follow the 4 channels. The first is 12.5 m long, the second 25 m while the remaining two channels are each 50 m apart. The total active streamer length for the EW96-05 cruise was 137.5 m(Fig. 3.2).

The optimal depth for a streamer in SCS studies is approximately 6m. This depth was maintained during the EW96-05 cruise through two items. The first is an oil filling in the streamer itself, which provides a neutral buoyancy. The second is the 156.75 meter kevlar tow leader, which provides the weight to keep the SCS streamer at its operating depth.

Recording system

The recording system that was aboard the R/V EWING during the EW96-05 cruise was the DSS-240 system. This system consists of a network of processors that make up subsystems that are each responsible for an aspect of recording the SCS data (Fig. 3.3). The recording process begins with the initiation of the shot cycle and ends with the writing of the SCS data to a storage tape.

Radio Data Link 3 (RDL3) is a multi-boat system controller in which the shot cycle originates (Fig. 3.4). RDL3 has the capability to control the shots of up to three seismic vessels. The firing rate during EW96-05 was controlled by a specified time interval. In order to so this, the RDL3 kept track of the time interval plus randomization and the Radio Event Synchronization System 2 (REVS2) within RDL3, initiated the shot cycle by sending the NAV Clock Prime (NCP) closure through the System Interface Board (SIB) to the Serial Line Interface Controller (SLIC). This occurs 312 ms after REVS2 has received closure from RDL3. The SLIC monitors such asynchronous serial devices as the air pressure monitor and streamer cable tension. This information is then sent to the RDL3.

After the SIB receives the NCP signal, the SIB conveys the signal to the Timing Analysis for Gun Synchronization (TAGS) engine (Fig. 3.5). The purpose of TAGS is to control the firing of the airgun array as well as to log the quality control information for each shot. When TAGS receives the signal from NCP, TAGS provides RDL3 with its setup and the source enable status. TAGS further gives source and array information to the Class Loop Automatic Source Synchronizer (CLASS) about when to fire the guns. Essentially, CLASS's responsibility is to fire the guns at precisely the correct time.

When RDL3 receives the source enable code from TAGS, it 'decides' on whether the guns should be fired. This is dependent on if the conditions for shooting have been met. If they have, then REVS2 sends a BLAST command to the CLASS. As soon as the guns have fired, CLASS generates a Time Break closure, sends it to the SIB and sends the measured firing times to TAGS. Tags in turn calculates which guns fired early or late and no fires. This data are sent to three places. The first is a monitor that displays the gun status. The second is the Control Executive Overseer (CEO), where a text-line printout shows that the shot times have been recorded. The third is the Ethernet Line Interface Controller (ELIC), which directs the information to the Cable Supervisor and Recording Unit (SCRU) in order that the data may be recorded on tape. The CEO is the user interface that is used in the real-time acquisition lab to program the CSRU.

If the SIB receives a Time Break closure, it generates a Time Break Echo (TBE), which is sent to RDL3. If this signal is not received by RDL3 within a certain time frame after receiving the Nav Clock signal, then the data for that particular shot are not recorded and an error is reported. RDL3 then receives the shot number, GPS recorded shot time and the ship location from SPECTRA. If the TBE receives its signal on time, the previous information is sent through the ELIC to the CSRU to be recorded in Trace 0 on the 3480 tape. In addition to this, the gun status for each shot is also recorded by the CSRU.

The seismic data is then digitized and sent to the Cable Subsystems (CSS) from the telemetry cans. It is then transferred to through the Hydrophone Array Sampling and Telemetry Electronics (HASTE) Personality module to the GPCC interface board where it is demultiplexed (Fig. 3.6). From the GPCC, the data are transferred by a VME bus to the PC Cable Data Display (PCDD) memory buffers. The VME is a high performance 32 but bus with a data through put bandwidth of 10 megabits/second. The high transfer rate is a function of the amount of data that are sent to the buffers with every shot. The most recent seismic data is then displayed by PCDD after the signal has been demultiplexed. The data are then displayed at a sample rate of 125 Hz. This is without an anti-aliasing filter, so aliasing is inevitable.

The PCDD contains 16 megabytes of memory, which is broken down into three buffers. One buffer consists of two six megabyte blocks and is used by the CSRU to stage the seismic data. While this is occurring, the PCDD is displaying the data and a SCSI splitter is copying the data from the VME side of the memory and recording it in SEG-D format on 3480 tapes. This is also occurring at the same time that the non-seismic data is entering the CSRU through a smaller GPIB bus (0.1 Mbit/second data throughput). This non-seismic data was the above mentioned data sent to the CSRU from the SLIC, ELIC, and CEO. The brute stack plots and near trace display require another copy of the seismic data, and these are plotted on two flatbed plotters.

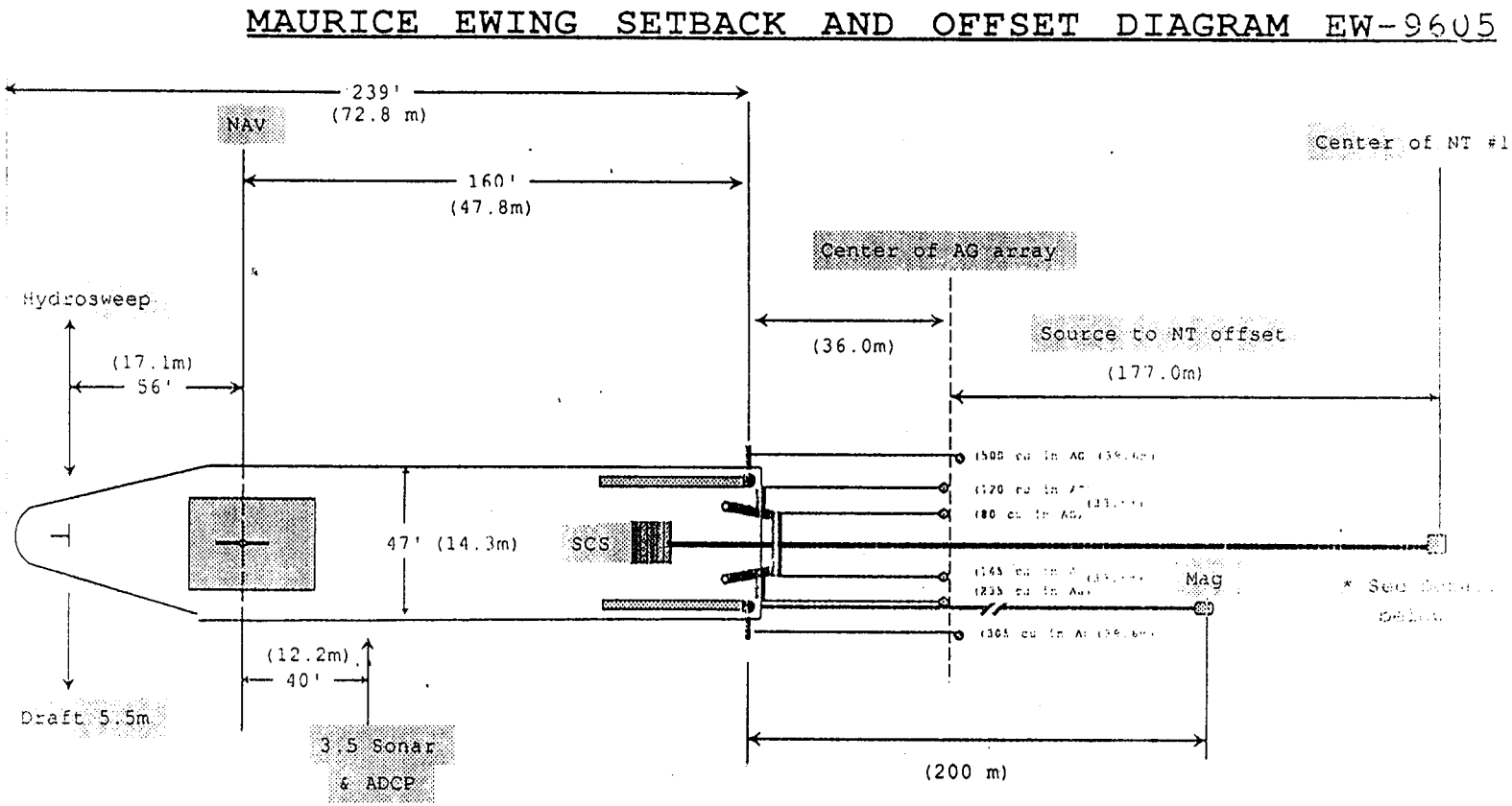

Figure 3.1. Setback and offset diagram for SCS reflection operations for MW96-05. Diagram also shows MR1 fish location and Magnetometer location.

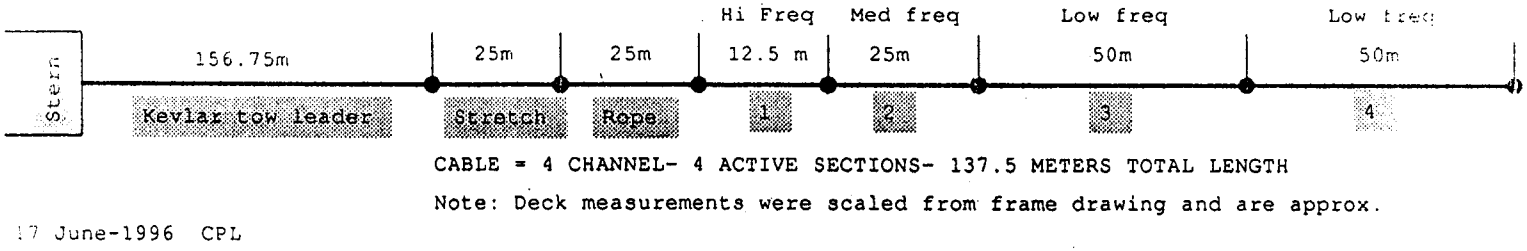

Figure 3.2 Sreamer configuration for SCS operations during MW96-05.

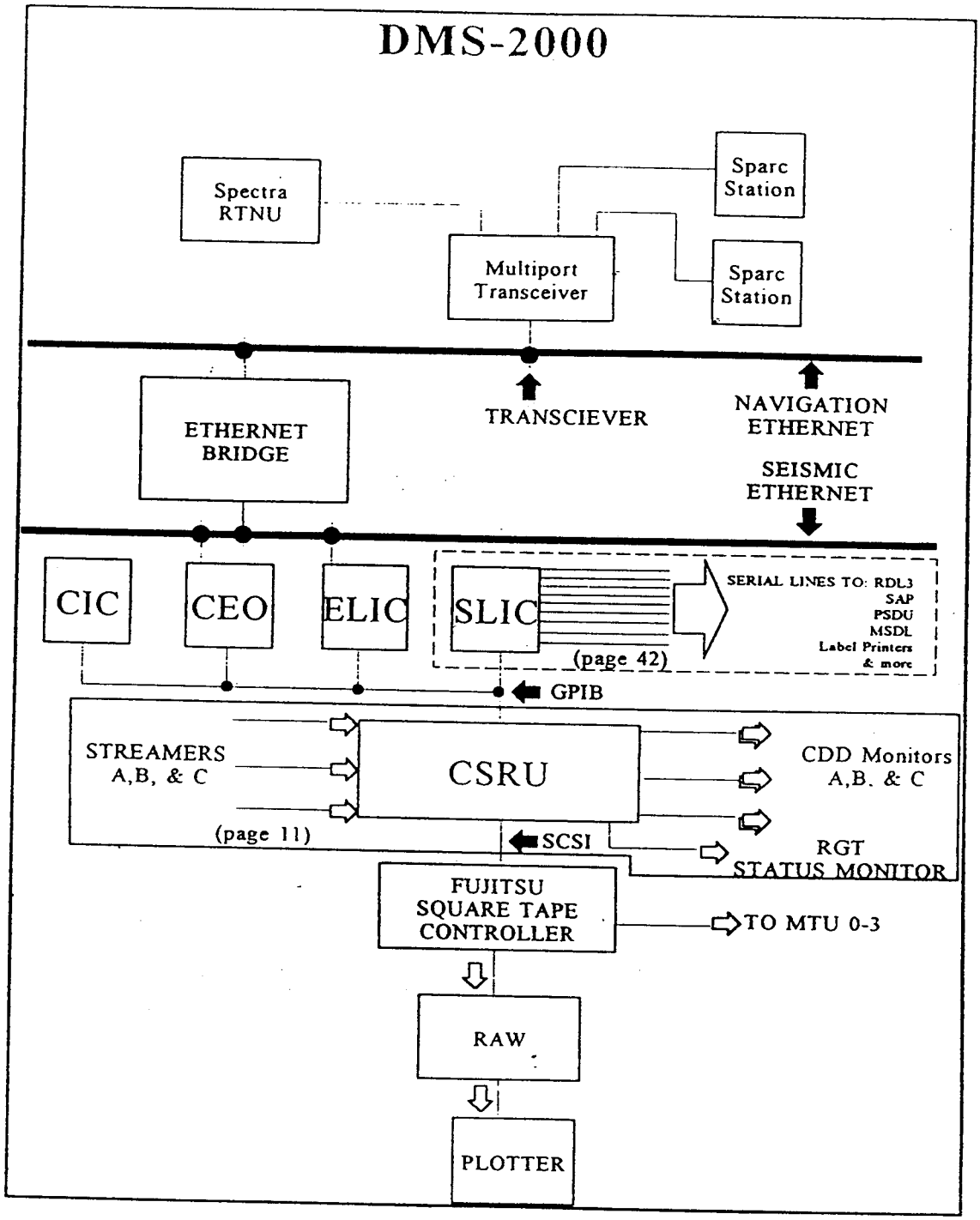

Figure 3.3. Schematic of DMS-2000 recording system. Although the *Ewing* is equipped with the newer DSS-240 system, overall similarities between the two systems allows the use of this diagram to explain the DSS-240.

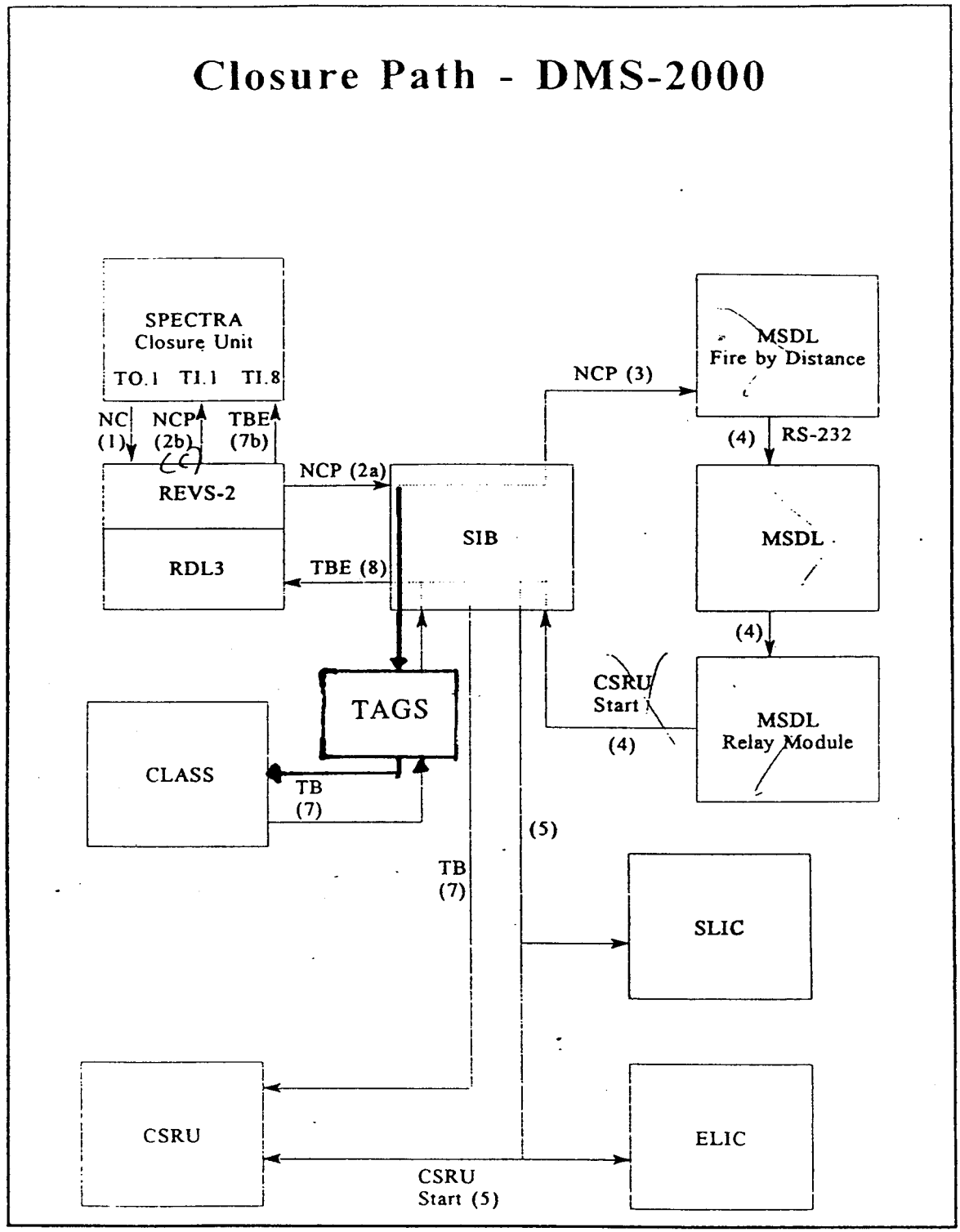

Figure 3.4. Shot cycle for DMS-2000 recording system. The DSS-240 system utilizes the TAGS subsystem in lieu of the MSDL, which was used in the older DMS-2000 system.

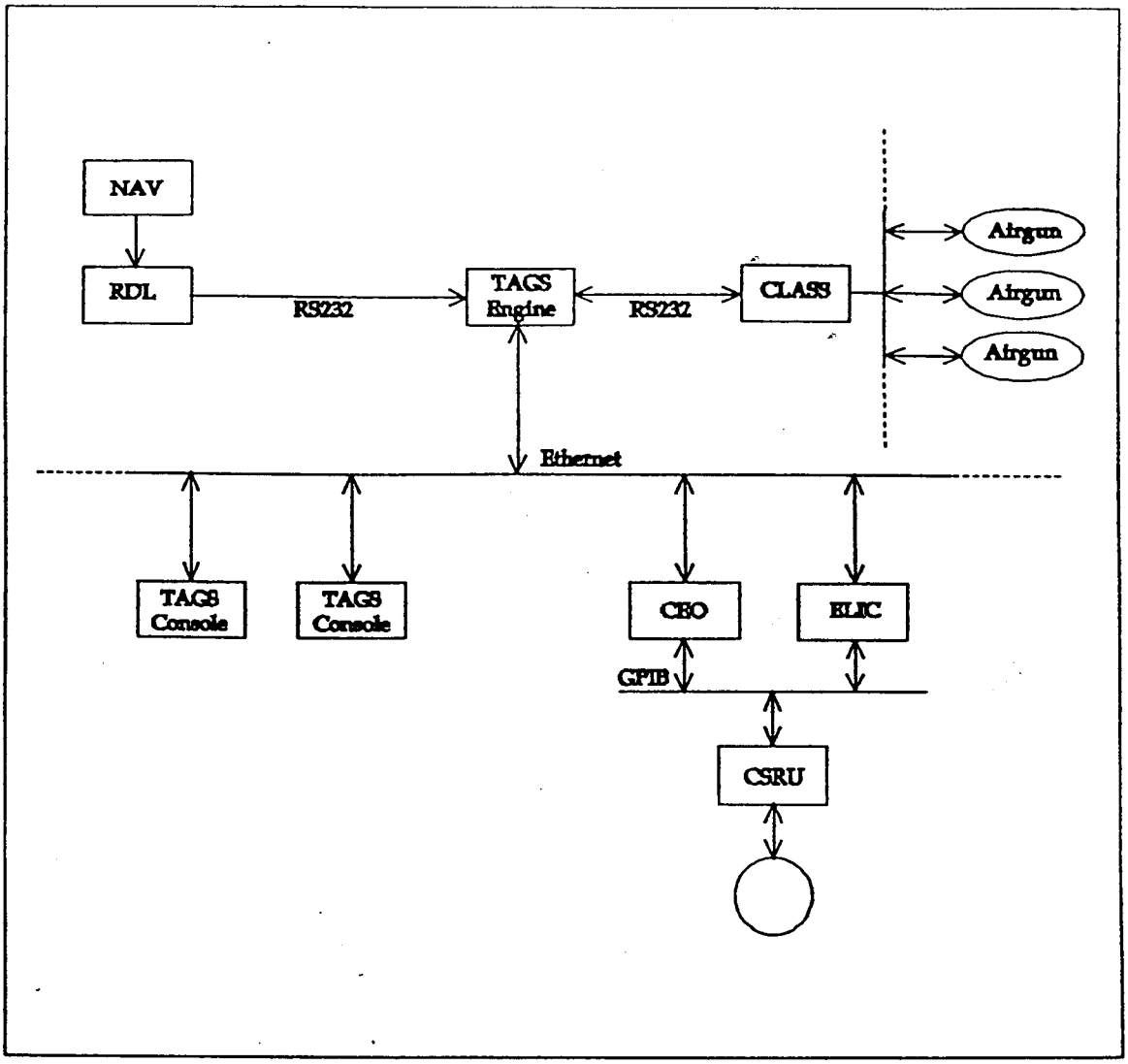

Figure 3.5. TAGS system integration and data flow for the DMS-2000. The DSS-240 has a similar data flow except that it does not receive the NC closure from navigation.

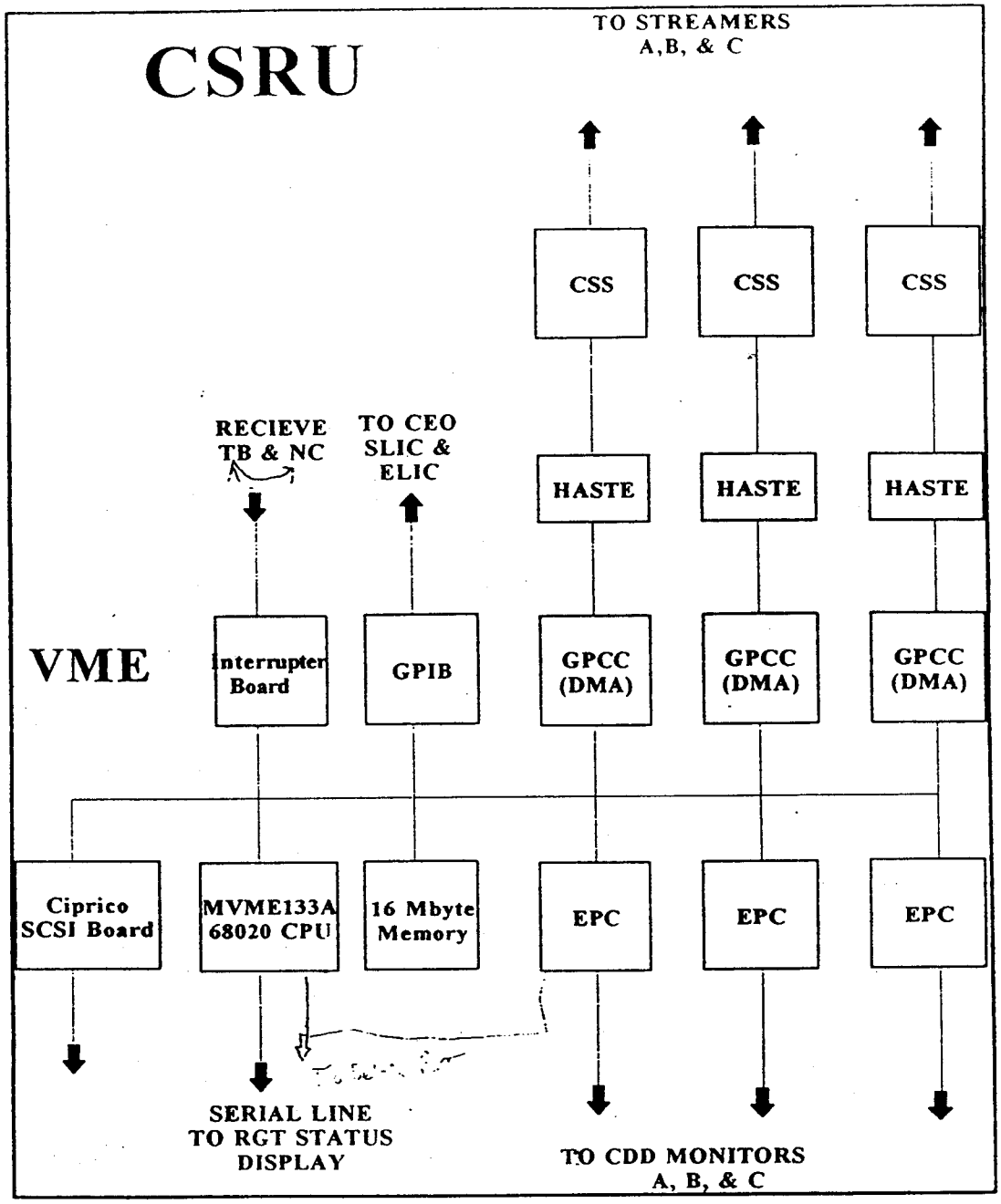

Figure 3.6 CSRU system for the older DMS-2000 system. DSS-240 has a comparable configuration.

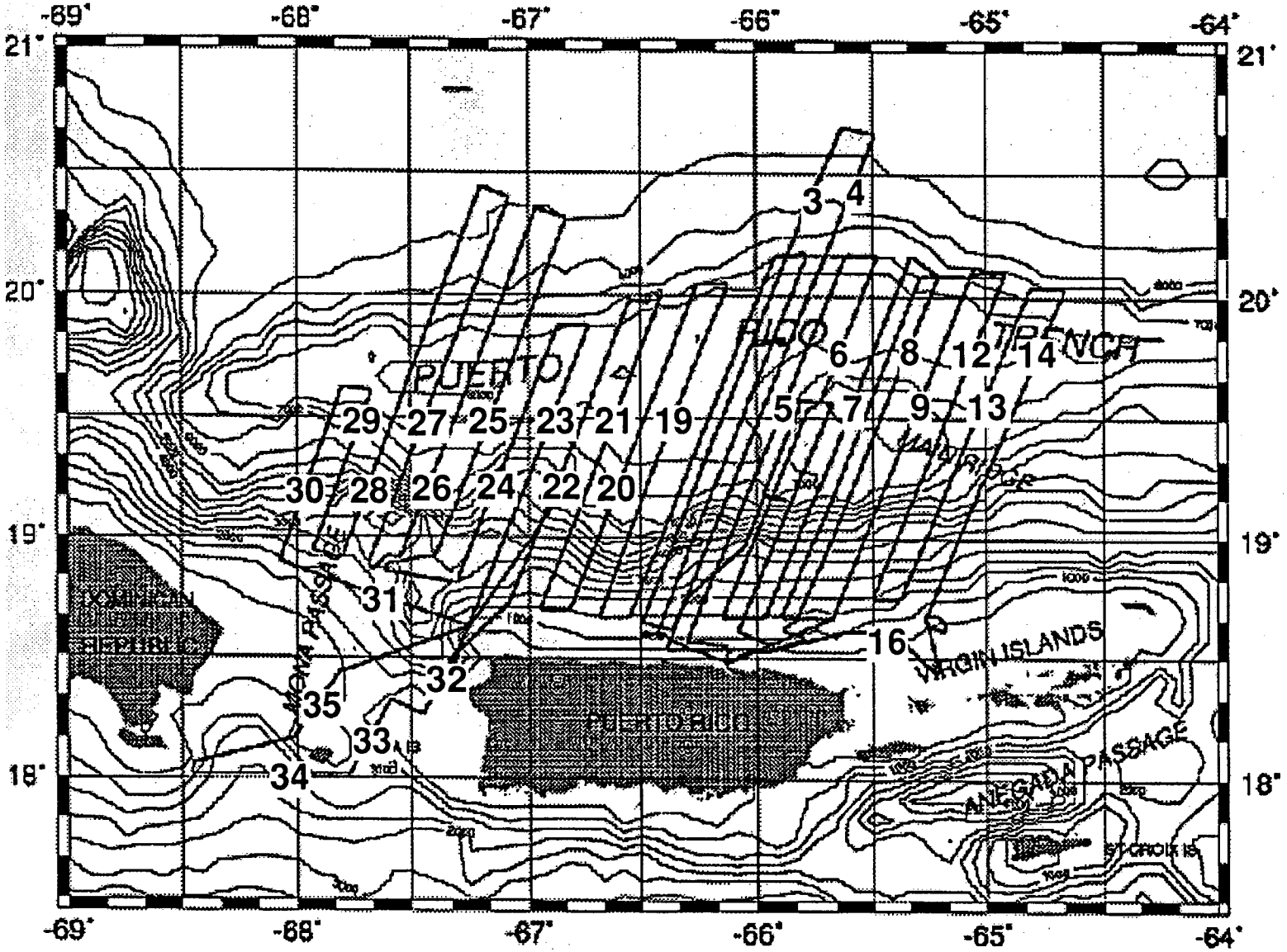

Figure 3.7 - SCS track lines for cruise EW96-05. MR1-only lines are unlabled

CHAPTER 4. AIRGUN CONFIGURATION

by John Charles III and Stefan Muszala

The air guns work by releasing pressurized air into the water creating a wave that travels through the water and bounce off interface changes in the sea floor. These waves bounce up and are received by the seismic streamer. Each gun contains a different amount of air that is released. This variation in size reduces the size of destructive interference or "bubble pulse" created by the air bubbles when the gun are fired. The gun works by filling a compartment with pressurized air then releasing the air suddenly by sending an electrical signal down a cord that is attached to the solenoid. The solenoid controls a small firing pin that releases the air (Figure 4.1).

During this survey we used a six gun array. One gun was mounted to a short boom attachment on the port and starboard booms and four guns where attached to the A-frame. The six guns used on this cruise where the 500, 305, 235, 145, 120, and 80 cubic inch air gun array. These numbers represent the cubic inches of air that the gun holds at 2000 psi. The entire array produces 1385 cubic inches of pressurized air at 2000 psi (Figure 4.2 & 4.3).

After the System Interface Board (SIB) receives the NAV Clock Prime (NCP) signal, the SIB conveys the signal to the Timing Analysis for Gun Synchronization (TAGS) engine (Figure 3.5). The purpose of TAGS is to control the firing of the airgun array as well as to log the quality control information for each shot, such as the depth of the airgun. This, for example, is supplied by a transducer mounted on each individual airgun. When TAGS receives the signal from NCP, TAGS provides Radio Data Link 3 (RDL3) with its setup and the source enable status. TAGS further gives source and array information to the Class Loop Automatic Source Synchronizer (CLASS) about when to fire the guns. Essentially, CLASS's responsibility is to fire the guns at precisely the correct time. When RDL3 receives the source enable code from TAGS, it 'decides' on whether the guns should be fired. If all of the conditions for shooting are met, then a signal is sent to the guns, and they are fired.

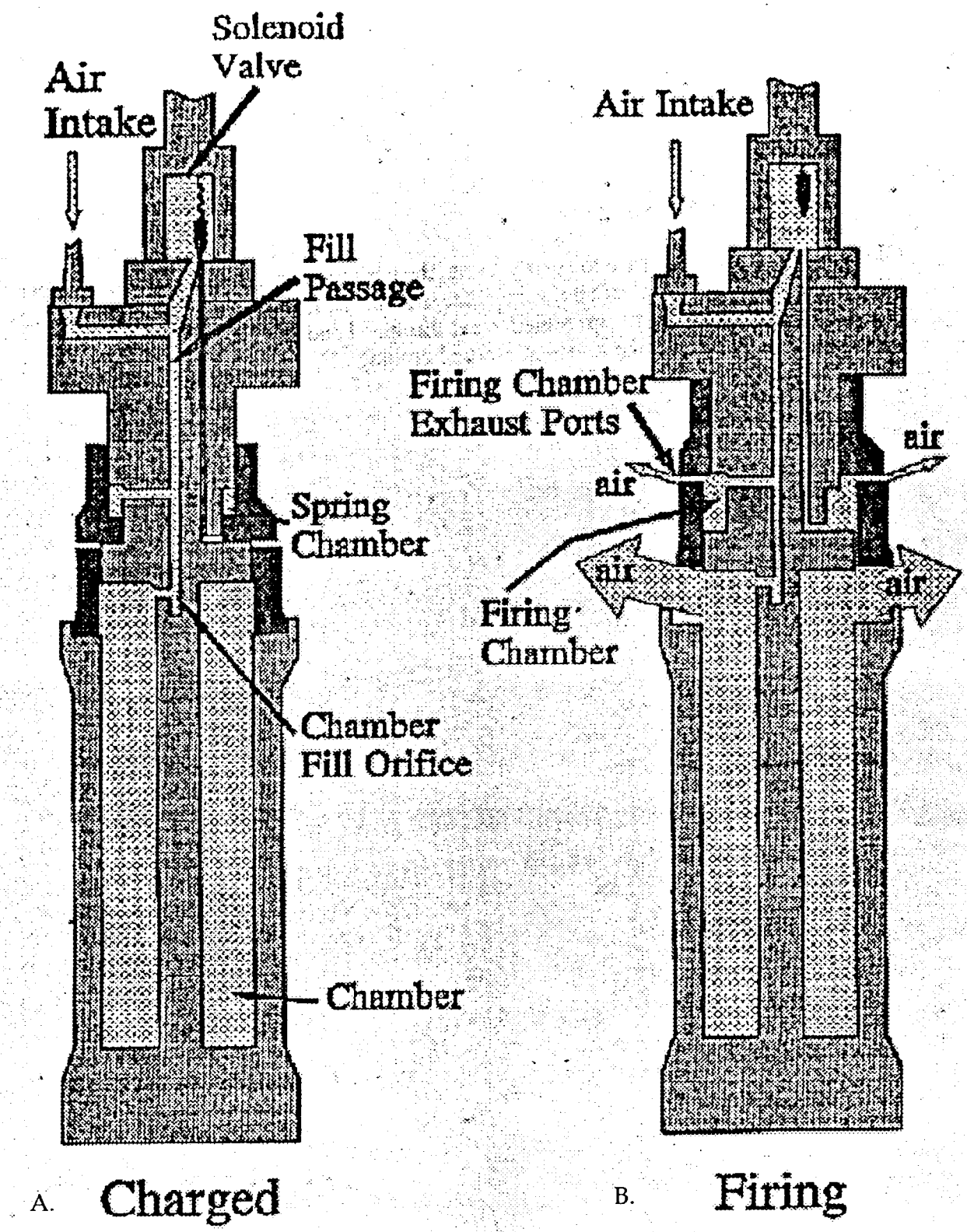

Figure 4.1 A. Is diagram of a charged air gun that is filled with air and at 2000 psi. B. Is a diagram of an air gun firing and releasing air into the water.

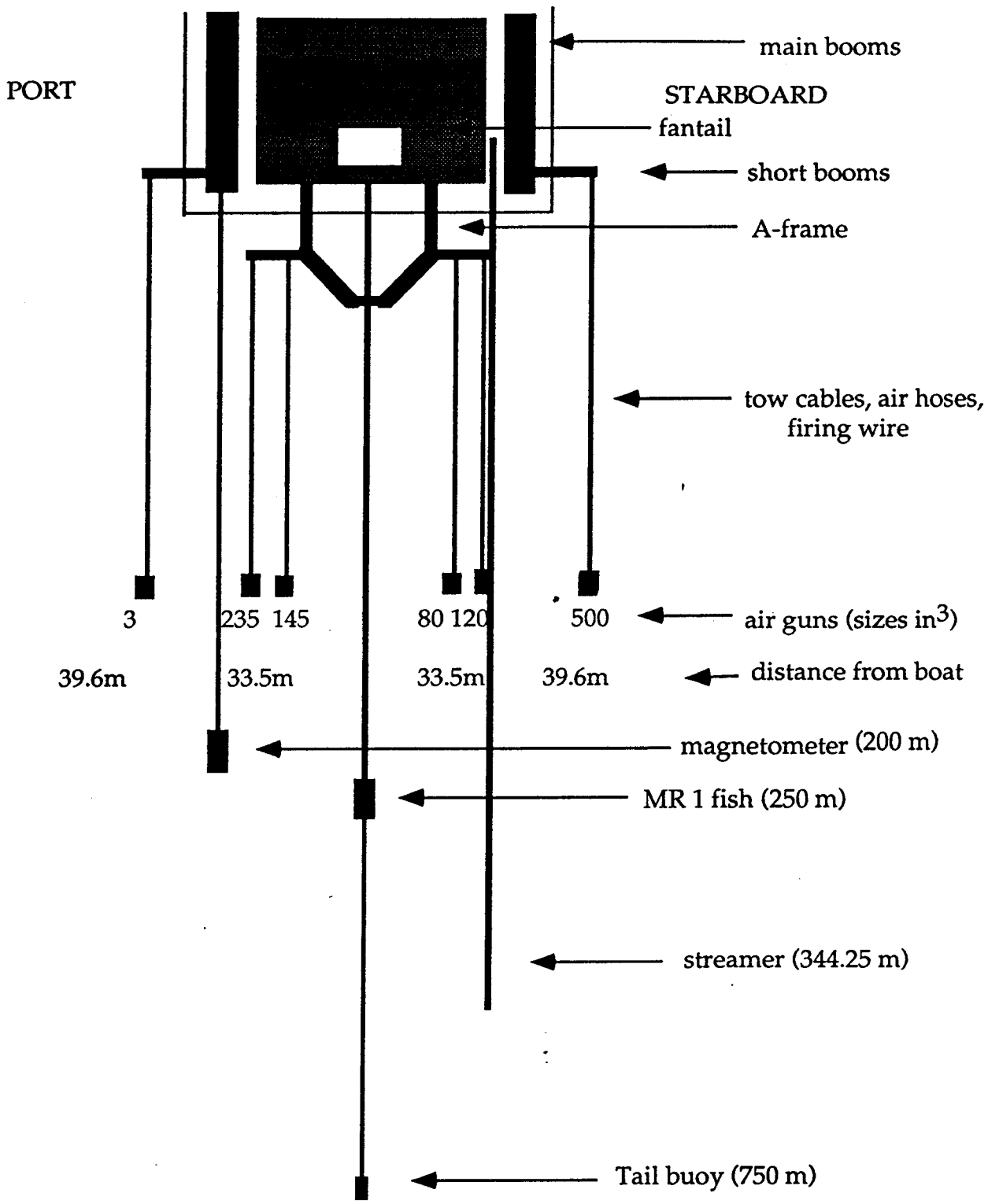

Figure 4. 2 The air gun array showing the six different air guns and where they are mounted. Diagram not drawn to scale.

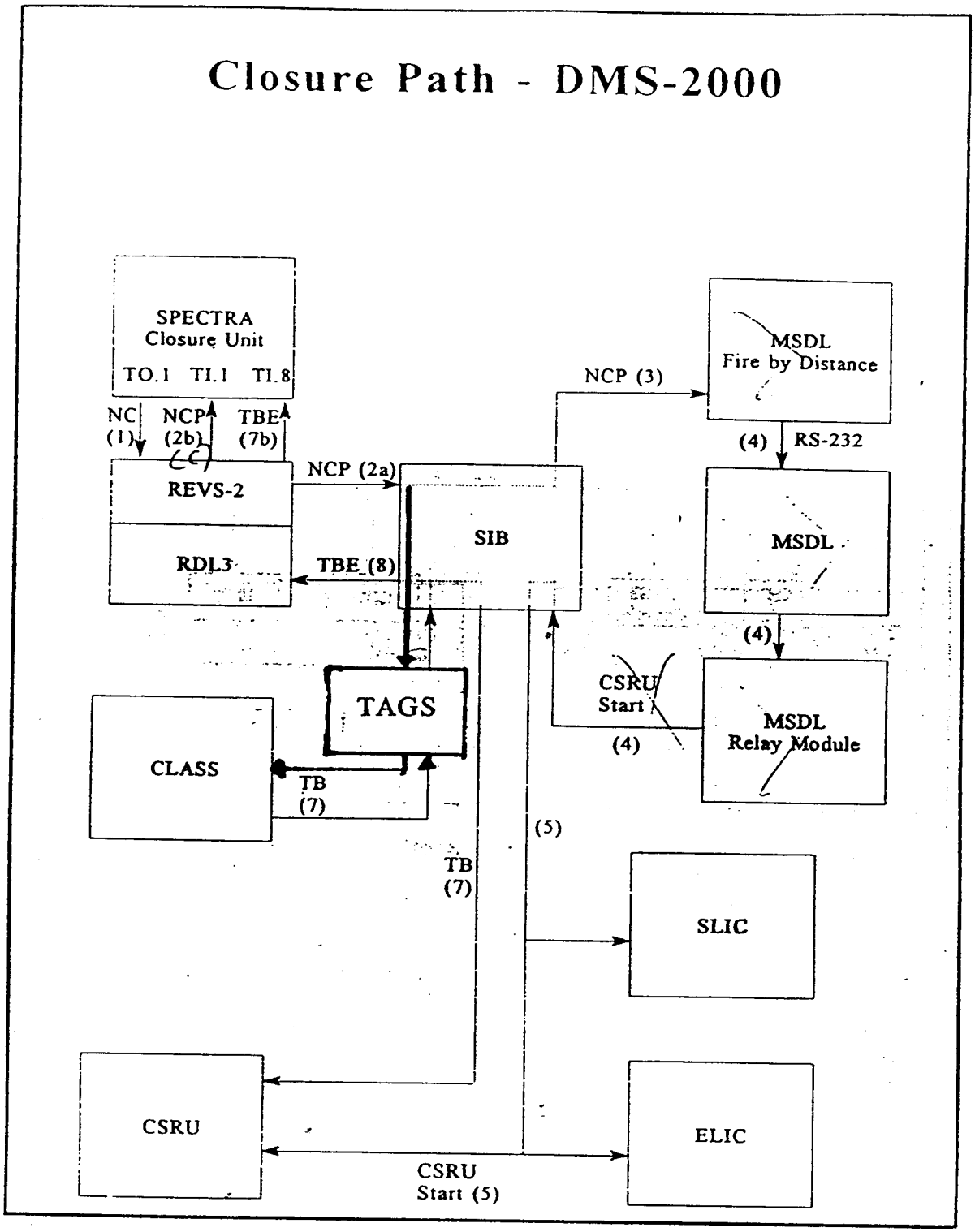

Figure 4. 3 - Shematic of shot time recording system used for SCS operations during EW96-05

Table 5.1

Single Channel Seismic data table

Line 1

start-point	JD 167	22.41'58"	18 40' 635 N	66 03' 118 W		SP 100
CC-point1	JD 168	08.19'	19 33' 957 N	65 42' 164 W		SP 2194
CC-point2	JD 168	09.18'	19 34' 08 N	65 48' 55 W		SP 2429
CC-point3	JD 168	18.15'	18 58' 240 N	66 02' 910 W		SP 3631
CC-point4	JD 168	21.32'	18 55' N	66 17' W	WP 59A	SP 4475
end-point	JD 168	23.02'59"	18 37' N	66 22' 0 W	WP 59	SP 4865
reelnumber	100	SP 100	SP 1002	902	10 sec.	prline1
reelnumber	101	SP 1003	SP 2002	999	10 sec.	prline1
reelnumber	102	SP 2003	SP 3003	1000	10 sec.	prline1
reelnumber	103	SP 3004	SP 3261	257	10 sec.	prline1
reelnumber	104	SP 3263	SP 4118	855	12 sec.	prlin1a
reelnumber	105	SP 4119	SP 4865	746	12 sec.'	prlin1a

In this line we made a several course changes.
CC 1 from 20 degrees to 285 degrees. CC 3 from 200 degrees to 227 degrees.
CC 2 from 285 degrees to 200 degrees. CC 4 from 227 degrees to 285 degrees.
During recording of line 1 we made a turn in the line. This was between 12 hrs. 55 min. and 16 hrs. 49 min.

Line 3

start-point	JD 168	23.21'22"	18 37' 957 N	66 25' 724 W		SP 4871
fin. turn-point	JD 169	00.32'	18 41' 192 N	66 28' 772 W	WP 56	SP 6689
end-point	JD 170	04.03'22"	20 41' 271 N	65 37' 748 W	WP 57B	SP 10698
reelnumber	106	SP 4871	SP 5727	856	12 sec.	prline3
reelnumber	107	no SP recorded on this reel				
reelnumber	108	SP 5729	SP 6586	857	12 sec.	prline3
reelnumber	109	SP 6587	SP 6683	96	12 sec.	prline3
reelnumber	110	SP 6689	SP 7544	855	14 sec.	prlin3a
reelnumber	111	SP 7545	SP 8275	730	14 sec.	prlin3a
reelnumber	112	SP 8278	SP 9133	855	14 sec.	prlin3a
reelnumber	113	no SP recorded on this reel				
reelnumber	114	SP 9135	SP 9990	855	14 sec.	prlin3b
reelnumber	115	SP 9991	SP 10698	707	14 sec.	prlin3b

Between line 3 or SP 6683 and line 3a or SP 6689 9 min. 25 sec. not recorded.
During recording of line 3 we made 2 turns in the line. The first turn was between SP 5870 and SP 6234.
The second turn was between SP 8276 and SP 8514.
Missing SP on line 3 : 5728, 6684-6688, 9134

Line 4

start-point	JD 170	04.14'01"	20 41' 271 N	65 37' 748 W		SP 10700
fin. turn-point	JD 170	05.21'	20 39' 31 N	65 29' 92 W	WP 60B	SP 10952
end-point	JD 171	04.29'13"	18 31' 09 N	66 21' 54 W		SP 16157
reelnumber	116	SP 10700	SP 11557	857	14 sec.	prline4
reelnumber	117	SP 11558	SP 12415	857	14 sec.	prline4
reelnumber	118	SP 12416	SP 13275	859	14 sec.	prline4
reelnumber	119	SP 13276	SP 14132	856	14 sec.	prline4
reelnumber	120	SP 14133	SP 14989	856	14 sec.	prline4
reelnumber	121	SP 14990	SP 15846	856	14 sec.	prline4
reelnumber	122	SP 15849	SP 16157	308	14 sec.	prline4

Missing SP on line 4 : 15847,15848

Line 5

start-point	JD 171	06.19'28"	18 32' 171 N	66 08' 524 W		SP 16160
fin. turn-point	JD 171	08.15'	18 34' 989 N	66 17' 454 W	WP 100	SP 16655
end-point	JD 172	01.43'34"	20 10' 003 N	65 33' 334 W	WP 101	SP 20736

reelnumber	123	SP 16160	SP 17015	855	12 sec.	prline5
reelnumber	124	SP 17016	SP 17872	856	12 sec.	prline5
reelnumber	125	SP 17873	SP 17973	100	12 sec.	prline5
reelnumber	126	SP 17975	SP 18832	857	14 sec.	prline5a
reelnumber	127	SP 18833	SP 19690	857	14 sec.	prline5a
reelnumber	128	SP 19691	SP 20548	857	14 sec.	prline5a
reelnumber	129	SP 20549	SP 20736	187	14 sec.	prline5a

Between line 5 or SP 17973 and line 5a or SP 17975 4 min. 30 sec. not recorded.
Missing SP on line 5 : 17974

Line 6

start-point	JD 172	01.50'43"	20 09' 986 N	65 32' 432 W	WP 101	SP 20738
fin. turn-point	JD 172	02.42'	20 09' 994 N	65 29' 45 W	WP 102	SP 20931
end-point	JD 172	18.54'03"	18 39' 993 N	66 07' 670 W	WP 103	SP 24544

reelnumber	130	SP 20738	SP 21594	856	14 sec.	prline6
reelnumber	131	no SP recorded on this reel				
reelnumber	132	SP 21596	SP 22451	855	14 sec.	prline6
reelnumber	133	SP 22452	SP 23308	856	14 sec.	prline6
reelnumber	134	SP 23309	SP 23624	315	14 sec.	prline6
reelnumber	135	SP 23626	SP 24482	856	12 sec.	prlin6a
reelnumber	136	no SP recorded on this reel				
reelnumber	137	SP 24484	SP 24544	60	12 sec.	prlin6a

Between line 6 or SP 23624 and line6a or SP 23626 8 min. 56 sec. not recorded
Missing SP on line 6 : 21595, 23645, 24483

In this line is a little shift	SP 22367	19 34' 572 N	65 43' 742 W
to the West between	SP 22600	19 29' 658 N	65 47' 604 W

Line 7

start-point	JD 172	19.04'59"	18 39' 993 N	66 07' 670 W	WP 103	SP 24546
fin. turn-point	JD 172	20.42'	18 40' 66 N	65 57' 78 W	WP 104	SP 24910
end-point	JD 173	12.37'47"	20 09' 526 N	65 19' 722 W	WP 105	SP 28470

reelnumber	138	SP 24546	SP 25403	857	12 sec.	prline7
reelnumber	139	no SP recorded on this reel				
reelnumber	140	SP 25405	SP 25641	236	12 sec.	prline7
reelnumber	141	SP 25643	SP 26500	857	14 sec.	prlin7a
reelnumber	142	SP 26501	SP 27357	856	14 sec.	prlin7a
reelnumber	143	SP 27358	SP 28214	856	14 sec.	prlin7a
reelnumber	144	SP 28215	SP 28470	255	14 sec.	prlin7a

Between line 7 or SP 25641 and line7a or SP 25643 6 min. 56 sec. not recorded
Missing SP on line 7 : 25404, 25642

Line 8

start-point	JD 173	12.45'47"	20 04' 649 N	65 18' 918 W	WP 105	SP 28472
fin. turn-point	JD 173	14.07'	20 04' 798 N	65 12' 798 W	WP 106	SP 28779
end-point	JD 174	05.21'52"	18 39' 837 N	65 49' 693 W	WP 107	SP 32334

reelnumber	145	SP 28472	SP 29327	855	14 sec.	prline8
reelnumber	146	no SP recorded on this reel				
reelnumber	147	SP 29329	SP 30184	855	14 sec.	prline8

reelnumber	148	SP 30185	SP 31042	857	14 sec.	prlin8a
reelnumber	149	SP 31043	SP 31190	147	14 sec.	prlin8a
reelnumber	150	SP 31191	SP 32047	856	12 sec.	prlin8a
reelnumber	151	no SP recorded on this reel				
reelnumber	152	SP 32049	SP 32334	285	12 sec.	prlin8a

Between line 8 or SP 28472 and line8a or SP 32334 4 min. 35 sec. not recorded
Missing SP on line 8 : 29328, 30225, 32048
SP with wrong numbers: 6477-6480 should be 29115-29118 and 7070-7078 should be 29708-29716

Line 9

start-point	JD 174	15.41'45"	18 45' 227 N	65 38' 606 W	WP 108	SP 32336
end-point	JD 175	06.04'41"	20 05'399 N	65 03' 753 W	WP 109	SP 35572

reelnumber	153	SP 32336	SP 33191	855	14 sec.	prline9
reelnumber	154	no SP recorded on this reel				
reelnumber	155	SP 33193	SP 34049	856	14 sec.	prline9
reelnumber	156	SP 34050	SP 34908	858	14 sec.	prline9
reelnumber	157	SP 34909	SP 35572	663	14 sec.	prline9

Missing SP on line 9 : 33192
SP with wrong numbers: 9863-9882 should be 32502-32522 and 9698-9699 should be 32337-32338

Line 10 and 11 only recorded MR 1 data.

Line 12

start-point	JD 176	08.54'55'	20 05' 01 N	64 58' 83 W		SP 35573
fin. turn-point	JD 176	09.34'	20 04' 001 N	64 55' 744 W	WP 112	SP 35722
end-point	JD 176	23.41'52"	18 45' 586 N	65 29' 730 W	WP 113	SP 38974

reelnumber	158	SP 35573	SP 36430	857	14 sec.	prline12
reelnumber	159	no SP recorded on this reel				
reelnumber	160	SP 36432	SP 37287	855	14 sec.	prline12
reelnumber	161	SP 37288	SP 37992	704	14 sec.	prline12
reelnumber	162	SP 37994	SP 38852	858	12 sec.	prlin12a
reelnumber	163	SP 37994	SP 38974	980	12 sec.	prlin12a

Missing SP on line 12 : 36431, 37993
Between line 12 or SP 37992 and line12a or SP 37994 11 min. 36 sec. not recorded
In the beginning of this line there is a lot of low-frequent noise in channel 4.

Line 13

start-point	JD 176	23.53'54"	18 44' 975 N	65 28' 937 W	WP 113	SP 38979
fin. turn-point	JD 177	00.57'	18 45' 492 N	65 22' 351 W	WP 114	SP 39250
end-point	JD 177	14.48'25"	20 01' 997 N	64 45' 016 W	WP 115	SP 42473

reelnumber	164	no SP recorded on this reel				
reelnumber	165	SP 38979	SP 39835	856	12 sec.	prline13
reelnumber	166	SP 39836	SP 40286	450	12 sec.	prline13
reelnumber	167	SP 40287	SP 41144	857	14 sec.	prline13
reelnumber	168	no SP recorded on this reel				
reelnumber	169	SP 41146	SP 42001	855	14 sec.	prlin13a
reelnumber	170	SP 42002	SP 42473	471	14 sec.	prlin13a

Missing SP on line 13 :41145
Between line 13 or SP 40286 and line13a or SP 40287 6 min. 37 sec. not recorded.
Reel 167, 169 and 170 give a "string is not a number" error when raeding out.

Line 14

start-point	JD 177	14.53'56"	20 02' 017 N	64 47' 374 W	WP 115	SP 42476
fin. turn-point	JD 177	16.30'	19 59' 590 N	64 40' 573 W	WP 116	SP 42835

end-point	JD 178	06.54'05"	18 39' 949 N	65 15' 894 W	WP 117	SP 1675
reelnumber	171	SP 42476	SP 43331	855	14 sec.	prline14
reelnumber	172	SP 43332	SP 44190	858	14 sec.	prline14
reelnumber	173	SP 44191	SP 44651	460	14 sec.	prline14
reelnumber	174	SP 100	SP 113	13	12 sec.	prlin14a
reelnumber	175	SP 114	SP 970	856	12 sec.	prlin14b
reelnumber	176	SP 971	SP 1675	704	12 sec.	prlin14b

Between line 14 or SP 44651 and line14a or SP 100 7 min. 34 sec. not recorded.
Reel 171, 172, 173 and 174 give a "string is not a number" error when raeding out.

Line 15

start-point	JD 178	07.01'01"	18 39' 191 N	65 15' 663 W		SP 1676
end-point	JD 178	07.06'37"	18 38' 747 N	65 15' 554 W		SP 1700
reelnumber	177	SP 1676	SP 1700	24	12 sec.	prline15
reelnumber	178	no SP recorded on this reel				

This line was cancelled right after the start because the people of the MR 1 were still busy.

Line 16

start-point	JD 178	08.40'30"	18 40' 82 N	65 13' 18 W	WP 117	SP 1705
CC-point	JD 178	11.39'	18 26' 955 N	65 14' 162 W	WP 118	SP 2471
end-point	JD 178	13.06'02"	18 33' 29 N	65 21' 01 W	WP 118A	SP 2843
reelnumber	179	SP 1705	SP 2560	855	12 sec.	prline16
reelnumber	180	SP 2561	SP 2843	282	12 sec.	prline16

In this line we made a course change from 170 degrees to 310 degrees.

Line 17 and 18 only recorded MR 1 data.

Line 19

start-point	JD 179	22.25'14"	18 39' 989 N	66 35' 938 W	WP 123	SP 2845
end-point	JD 180	14.11'29"	20 03' 270 N	66 08' 016 W	WP 124	SP 6485
reelnumber	181	SP 2845	SP 3678	833	12 sec.	prline19
reelnumber	182	SP 3680	SP 4535	855	14 sec.	prlin19a
reelnumber	183	no SP recorded on this reel				
reelnumber	184	SP 4537	SP 5392	855	14 sec.	prlin19a
reelnumber	185	SP 5393	SP 6249	856	14 sec.	prlin19a
reelnumber	186	SP 6250	SP 6485	235	14 sec.	prlin19a

Between line 19 or SP 3678 and line19a or SP 3680 3 min. 35 sec. not recorded.
Missing SP on line 19 :3679, 4536

Line 20

start-point	JD 180	14.40'41"	20 03' 010 N	66 10' 801 W	WP 124	SP 6490
fin. turn-point	JD 180	15.21'	20 02' 522 N	66 15' 193 W	WP 125	SP 6642
end-point	JD 181	06.09'29"	18 42' 012 N	66 50' 774 W	WP 126	SP 10050
reelnumber	187	SP 6490	SP 7347	857	14 sec.	prlin20a
reelnumber	188	SP 7348	SP 8204	856	14 sec.	prlin20a
reelnumber	189	SP 8205	SP 9061	856	14 sec.	prlin20a
reelnumber	190	SP 9062	SP 9303	241	14 sec.	prlin20a
reelnumber	191	SP 9304	SP 10050	746	12 sec.	prlin20b

Between line 20a or SP 9303 and line20b or SP 6642 4 min. 36 sec. not recorded.

Line 21

start-point	JD 181	06.16'02"	18 41' 991 N	66 51' 051 W	WP 126	SP 10053
fin. turn-point	JD 181	07.14'	18 42' 371 N	66 56' 750 W	WP 127	SP 10305

end-point	JD 181	20.48'29"	19 59' 038 N	66 25' 571 W	WP 128	SP 13440
reelnumber	192	SP 10053	SP 10909	856	12 sec.	prline21
reelnumber	193	SP 10910	SP 11208	298	12 sec.	prline21
reelnumber	194	SP 11211	SP 12068	857	14 sec.	prlin21a
reelnumber	195	SP 12069	SP 12926	857	14 sec.	prlin21a
reelnumber	196	SP 12927	SP 13439	512	14 sec.	prlin21a

Between line 21 or SP 11209 and line21a or SP 11210 8 min. 49 sec. not recorded.
Missing SP on line 21: 12070, 11209, 11210.

Line 22

start-point	JD 181	20.56'16"	19 59' 038 N	66 25' 571 W	WP 128	SP 13443
fin. turn-point	JD 181	22.08'	19 58' 344 N	66 33' 210 W	WP 129	SP 13716
CC-point	JD 182	11.40'	18 43' 978 N	67 04' 983 W	WP 130	SP 16802
end-point	JD 182	15.53'22"	18 28' 368 N	67 19' 494 W	WP 131	SP 17887
reelnumber	198	no SP recorded on this reel				
reelnumber	199	SP 13443	SP 14299	856	14 sec.	prline22
reelnumber	200	no SP recorded on this reel				
reelnumber	201	SP 14301	SP 15156	855	14 sec.	prline22
reelnumber	202	SP 15157	SP 15943	786	14 sec.	prline22
reelnumber	203	SP 15944	SP 16800	856	12 sec.	prlin22b
reelnumber	204	SP 16801	SP 17658	857	12 sec.	prlin22b
reelnumber	205	SP 17659	SP 17887	228	12 sec.	prlin22b

Between line 22 or SP 15943 and line22b or SP 15944 17 min. 4 sec. not recorded.
Missing SP on line 22 :13441, 13442, 14300
In this line we made a course change from 220 degrees to 230 degrees.

Line 23

start-point	JD 182	16.30'10"	18 30' 199 N	67 18' 721 W	WP 131	SP 17885
end-point	JD 183	07.11'56"	19 52' 979 N	66 44' 973 W	WP 132	SP 21516
reelnumber	206	SP 17888	SP 18744	856	12 sec.	prlin23a
reelnumber	207	SP 18745	SP 19601	856	12 sec.	prlin23a
reelnumber	208	SP 19602	SP 19843	241	12 sec.	prlin23a
reelnumber	209	SP 19844	SP 20701	857	14 sec.	prlin23b
reelnumber	210	SP 20702	SP 21516	814	14 sec.	prlin23b

Between line 23a or SP 19601 and line23b or SP 19602 6 min. 44 sec. not recorded.

Line 24

start-point	JD 183	07.16'11"	19 52' 912 N	66 45' 625 W	WP 132	SP 21517
fin. turn-point	JD 183	08.24'	19 52' 330 N	66 52' 217 W	WP 133	SP 21772
CC-point	JD 183	19.54'	18 48' 809 N	66 18' 759 W	WP 134	SP 24487
end-point	JD 183	22.45'26"	18 52' 549 N	66 44' 973 W	WP 135B	SP 25223
reelnumber	211	SP 21517	SP 22375	858	14 sec.	prlin24a
reelnumber	212	no SP recorded on this reel				
reelnumber	213	SP 22377	SP 23233	856	14 sec.	prlin24a
reelnumber	214	SP 23234	SP 23316	82	14 sec.	prlin24a
reelnumber	215	SP 23319	SP 24175	856	12 sec.	prlin24b
reelnumber	216	no SP recorded on this reel				
reelnumber	217	SP 24177	SP 25032	855	12 sec.	prlin24b
reelnumber	218	SP 25033	SP 25223	190	12 sec.	prlin24b

Between line 24 or SP 23317 and line 24b or SP 23318 5 min. 17 sec. not recorded.
Missing SP on line 24 : 22376, 23317, 23318, 24176.
In this line we made a course change from 220 degrees to 280 degrees.

Line 25

start-point	JD 183	22.51'30"	18 51'925 N	67 36' 486 W	WP 135B	SP 25224
fin. turn-point	JD 183	23.10'	18 53' 392 N	67 35' 696 W	WP 135C	SP 25304
CC-point	JD 183	01.07'	18 55' 725 N	67 23' 725 W	WP 135D	SP 25809
end-point	JD 184	16.09'16"	20 19'852 N	66 53' 216 W	WP 136	SP 29216

reelnumber	219	SP 25224	SP 26080	856	12 sec.	prline25
reelnumber	220	SP 26081	SP 26179	98	12 sec.	prline25
reelnumber	221	SP 26180	SP 27039	859	14 sec.	prlin25b
reelnumber	222	no SP recorded on this reel				
reelnumber	223	SP 27041	SP 27897	856	14 sec.	prlin25b
reelnumber	224	SP 27898	SP 28754	856	14 sec.	prlin25b
reelnumber	225	SP 28755	SP 29215	460	14 sec.	prlin25b

In this line we made a course change from 80 degrees to 20 degrees.
Between line 25 or SP 26179 and line 25b or SP 26180 5 min. 36 sec. not recorded.
Missing SP on line 25 : 26181, 26182, 27040.
In this line we did a noise test. This was between SP 29147 and SP 29182.

Line 26

start-point	JD 184	16.14'40"	20 20' 053 N	66 53' 776 W	WP 136	SP 29218
fin. turn-point	JD 184	16.56'	20 21' 063 N	66 57' 973 W	WP 137	SP 29374
end-point	JD 185	07.41'27"	18 54' 990 N	67 33' 541 W	WP 138	SP 32213

reelnumber	226	no SP recorded on this reel				
reelnumber	227	SP 29218	SP 29725	507	14 sec.	prline26
reelnumber	228	SP 29734	SP 30590	856	14 sec.	prlin26b
reelnumber	229	SP 30591	SP 31178	587	14 sec.	prlin26b
reelnumber	230	SP 31180	SP 32035	855	14 sec.	prlin26c
reelnumber	231	no SP recorded on this reel				
reelnumber	232	SP 32037	SP 32213	176	14 sec.	prlin26c

Missing SP on line 26 : 29726-29733, 31179, 32036.
Between line 26 or SP 29725 and line 26b or SP 29726 1 hrs. 08 min. not recorded.
Between line 26b or SP 31178 and line 26c or SP 31179 1 hrs. 02 min. not recorded.

Line 27

start-point	JD 185	07.48'01"	18 55' 223 N	67 34' 186 W	WP 138	SP 32214
fin. turn-point	JD 185	9.09'	18 53' 021 N	67 41' 054 W	WP 139	SP 32520
end-point	JD 186	00.55'12"	20 24' 280 N	67 05' 306 W	WP 140	SP 35530

reelnumber	233	SP 32214	SP 33070	856	14 sec.	prlin27a
reelnumber	234	no SP recorded on this reel				
reelnumber	235	SP 33072	SP 33652	580	14 sec.	prlin27a
reelnumber	236	no SP recorded on this reel				
reelnumber	237	no SP recorded on this reel				
reelnumber	238	SP 33663	SP 33686	23	18 sec.	prlin27d
reelnumber	239	SP 33690	SP 34440	750	18 sec.	prlin27e
reelnumber	240	SP 34441	SP 35191	750	18 sec.	prlin27e
reelnumber	241	SP 35192	SP 35530	338	18 sec.	prlin27e

Missing SP on line 27 : 33071, 33653-3362, 33667,33668.
Between line 27a or SP 33652 and line 27d or SP 33663 17 min. 51 sec. not recorded.
Between line 27d or SP 33686 and line 27e or SP 33690 6 min. not recorded.
In the beginning of this line we made an extra turn south.
In SP 32290 at 8.08' we changed course to 290 grs and in SP 32520 at 9.19' we came on line 27 in WP 139.

Line 28

start-point	JD 186	00.58'33"	20 24' 380 N	67 05' 630 W	WP 140	SP 35531
fin. turn-point	JD 186	9.09'	20 26' 148 N	67 12' 488 W	WP 141	SP 35787
end-point	JD 186	17.55'05"	18 55' 001 N	67 48' 870 W	WP 142	SP 39343

reelnumber	242	SP 35531	SP 36388	857	14 sec.	prline28
reelnumber	243	SP 36389	SP 37245	856	14 sec.	prline28
reelnumber	244	SP 37246	SP 38102	856	14 sec.	prline28
reelnumber	245	SP 38103	SP 38959	856	14 sec.	prline28
reelnumber	246	SP 38960	SP 39343	383	14 sec.	prline28

Line 29

start-point	JD 186	18.01'36"	18 55'176 N	67 49' 580 W	WP 142	SP 39346
fin. turn-point	JD 186	18.01'	18 57' 561 N	67 55' 367 W	WP 143	SP 39585
end-point	JD 187	01.45'20"	19 35' 938 N	67 40' 375 W	WP 144	SP 41085

reelnumber	247	no SP recorded on this reel				
reelnumber	248	SP 39346	SP 40202	856	14 sec.	prline29
reelnumber	249	no SP recorded on this reel				
reelnumber	250	SP 40204	SP 41059	855	14 sec.	prline29
reelnumber	251	SP 41060	SP 41085	25	14 sec.	prline29

Missing SP on line 29 : 40203.

Line 30

start-point	JD 187	02.01'32"	19 36' 782 N	67 42' 171 W	WP 144	SP 39346
fin. turn-point	JD 187	03.00'	19 36' 674 N	67 48' 251 W	WP 145	SP 39585
end-point	JD 187	09.52'28"	18 54' 538 N	68 04' 433 W	WP 146	SP 41085

reelnumber	252	no SP recorded on this reel				
reelnumber	253	SP 41088	SP 41943	855	14 sec.	prline30
reelnumber	254	SP 41944	SP 42800	856	14 sec.	prline30
reelnumber	255	SP 42801	SP 42854	53	14 sec.	prline30

Missing SP on line 29 : 40203.
Speed up to 6.6 knots.

Line 31

start-point	JD 187	10.01'23"	18 53' 753 N	68 03' 791 W	WP 146	SP 42858
end-point	JD 187	17.29'56"	18 37' 265 N	67 15' 061 W	WP 147	SP 44517

reelnumber	256	no SP recorded on this reel				
reelnumber	257	SP 42858	SP 42889	31	12 sec.	prline31
reelnumber	258	SP 42889	SP 43745	856	12 sec.	prlin31a
reelnumber	259	SP 43746	SP 44517	771	12 sec.	prlin31a

The pop rate was 16 sec. in stead of 14. sec.
Between line 21 or SP 42889 and line 31a or SP 42889 7 min. 11 sec. not recorded.

Line 32

start-point	JD 187	17.33'59"	18 37' 043 N	67 15' 444 W	WP 147	SP 44518
end-point	JD 187	21.22'15"	18 16' 571 N	67 28' 777 W	WP 148	SP 45377

reelnumber	260	SP 44518	SP 45377	859	12 sec.	prline32

The pop rate was 16 sec. in stead of 14. sec.

Line 33

start-point	JD 188	00.07'36"	18 10' 210 N	67 40' 681 W		SP 45389
end-point	JD 188	01.41'52"	18 01' 229 N	67 45' 883 W	WP 150	SP 45741
reelnumber	261	no SP recorded on this reel				
reelnumber	262	no SP recorded on this reel				
reelnumber	263	SP 45389	SP 45741	352	14 sec.	prline33

Line 34

start-point	JD 188	01.45'34"	18 00' 955 N	67 46' 226 W	WP 150	SP 45744
end-point	JD 188	08.09'56"	18 01' 870 N	68 27' 086 W	WP 151	SP 47185
reelnumber	263	SP 45744	SP 46600	856	14 sec.	prline34
reelnumber	264	no SP recorded on this reel				
reelnumber	265	SP 46602	SP 47185	583	14 sec.	prline34

Missing SP on line 34 : 46601.

Line 35

start-point	JD 188	08.20'48"	18 02' 791 N	68 27' 086 W	WP 151	SP 47186
fin. turn-point	JD 188	8.33'	18 03' 71 N	68 26' 59 W	WP 152	SP 47243
CC-point	JD 188	13.20'	18 15' 402 N	67 56' 176 W	WP 153	SP 48472
CC-point	JD 188	15.20'	18 26' 299 N	67 48' 705 W	WP 154	SP 49000
end-point	JD 188	20.00'48"	18 38' 015 N	67 15' 240 W	WP 155	SP 50186
reelnumber	266	SP 47186	SP 48043	857	12 sec.	prlin35b
reelnumber	267	SP 48044	SP 48900	856	12 sec.	prlin35b
reelnumber	268	SP 48901	SP 49758	857	12 sec.	prlin35b
reelnumber	269	SP 49759	SP 50186	427	12 sec.	prlin35b

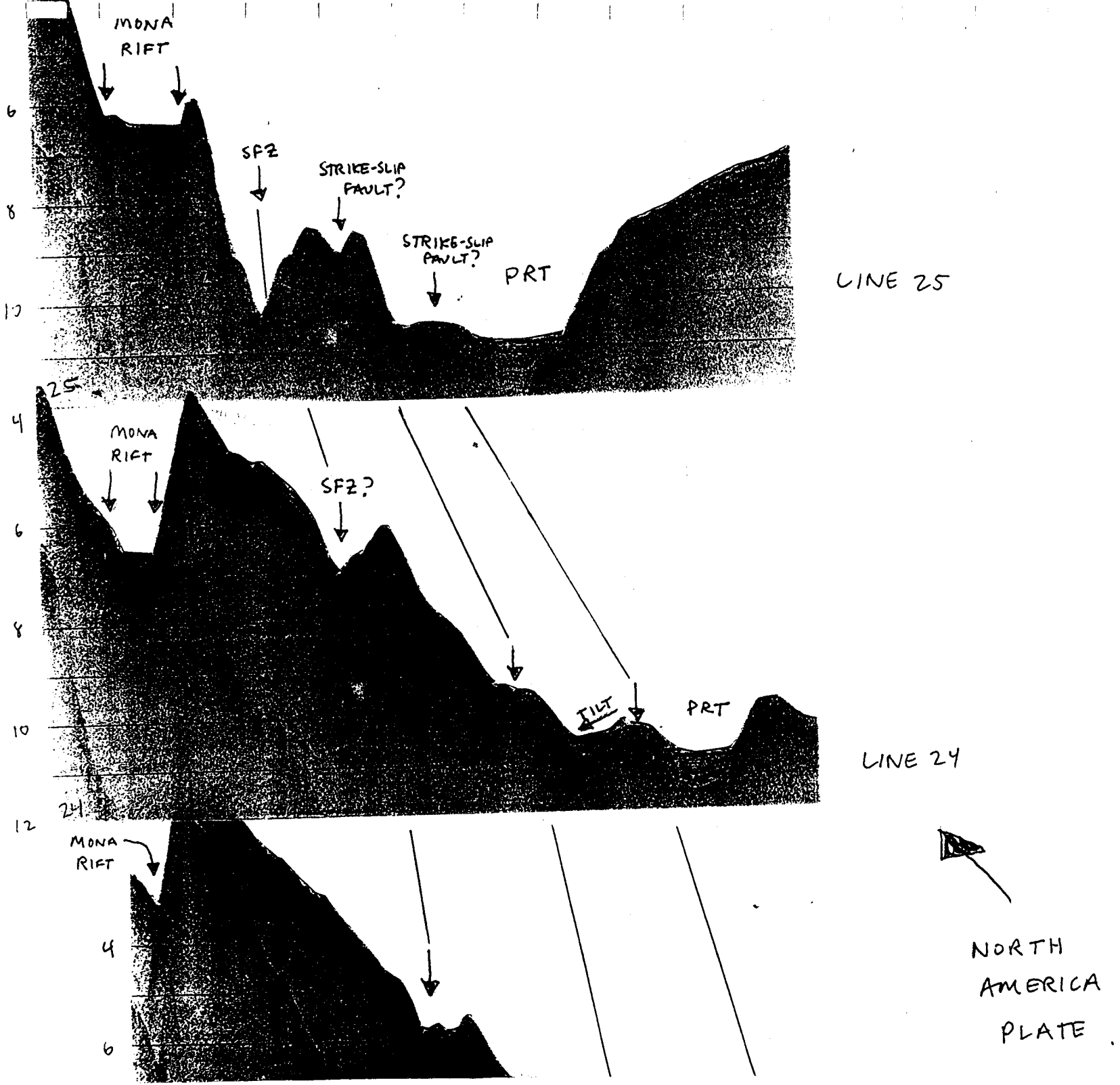
MONA RIFT
SFZ
STRIKE-SLIP FAULT?
STRIKE-SLIP FAULT?
PRT
LINE 25
MONA RIFT
SFZ?
TILT
PRT
LINE 24
MONA RIFT
NORTH AMERICA PLATE